AD_____

Award Number: DAMD17-98-1-8334

TITLE: Innovative Approaches for Determining the Role of BRCA2 and BRCA1 in DNA Recombinational Repair: Examination of Genetic Instability and Possible Therapeutic Uses

PRINCIPAL INVESTIGATOR: Maria Jasin, Ph.D.

CONTRACTING ORGANIZATION: Sloan-Kettering Institute for Cancer Research
New York, New York 10021

REPORT DATE: December 2001

TYPE OF REPORT: Final

PREPARED FOR: U.S. Army Medical Research and Materiel Command
Fort Detrick, Maryland 21702-5012

REPORT DOCUMENTATION PAGE

Form Approved
OMB No. 074-0188

1. AGENCY USE ONLY (Leave blank)	2. REPORT DATE	3. REPORT TYPE AND DATES COVERED
	December 2001	Final (1 Dec 98 - 30 Nov 01)

4. TITLE AND SUBTITLE
Innovative Approaches for Determining the Role of BRCA2 and BRCA1 in DNA Recombinational Repair: Examination of Genetic Instability and Possible Therapeutic Uses

5. FUNDING NUMBERS
DAMD17-98-1-8334

6. AUTHOR(S)
Maria Jasin, Ph.D.

7. PERFORMING ORGANIZATION NAME(S) AND ADDRESS(ES)
Sloan-Kettering Institute for Cancer Research
New York, New York 10021

E-Mail: m-jasin@ski.mskcc.org

8. PERFORMING ORGANIZATION REPORT NUMBER

9. SPONSORING / MONITORING AGENCY NAME(S) AND ADDRESS(ES)
U.S. Army Medical Research and Materiel Command
Fort Detrick, Maryland 21702-5012

10. SPONSORING / MONITORING AGENCY REPORT NUMBER

11. SUPPLEMENTARY NOTES

12a. DISTRIBUTION / AVAILABILITY STATEMENT
Approved for Public Release; Distribution Unlimited

12b. DISTRIBUTION CODE

13. ABSTRACT ***(Maximum 200 Words)***

Direct evidence for the involvement of the hereditary breast cancer genes BRCA1 and BRCA2 in the repair of chromosomal double-strand breaks by homologous recombination (i.e., homology-directed repair or HDR) is provided. HDR is a precise form of repair, whereas misrepair of breaks by other mechanisms compromises genomic integrity. Key to HDR pathways in mammalian cells is the Rad51 strand-exchange protein. Since the BRCA proteins interact with Rad51, we proposed that HDR is defective in cells deficient for these proteins. In this final report we describe homologous gene-targeting experiments in Brca1 and Brca2-deficient ES cells that bring in an HDR substrate containing green fluorescent protein gene repeats. Firstly, gene targeting is reduced in both cell lines although with differential effects. Secondly, repair of an induced break in the HDR, as monitored by measuring green fluorescence within the cell, is reduced in both cell lines to a similar extent. Thirdly, Brca1 deficiency causes hypersensitivity to mitomycin C but this sensitivity is correctable. Fourthly, in wild-type cells, we see an HDR defect by interfering with Rad51 by expressing a peptide from Brca2. Defects in HDR in Brca mutants may contribute to the development of early-onset breast and ovarian cancers by destabilizing the genome.

14. SUBJECT TERMS
Breast Cancer, BRCA2, homologous recombination, homologous repair, double-strand breaks, BRCA1

15. NUMBER OF PAGES
34

16. PRICE CODE

17. SECURITY CLASSIFICATION OF REPORT	18. SECURITY CLASSIFICATION OF THIS PAGE	19. SECURITY CLASSIFICATION OF ABSTRACT	20. LIMITATION OF ABSTRACT
Unclassified	Unclassified	Unclassified	Unlimited

TABLE OF CONTENTS

INTRODUCTION

In mammals, like other organisms, homologous recombination contributes to the maintenance of the integrity of the genome. For example, homologous recombination can be used to precisely repair lesions such as chromosomal double-strand breaks (DSBs) (i.e., homology-directed repair or HDR). Sister chromatids are the most common repair template, since they are identical (1). In mammalian cells, HDR was thought to be disfavored relative to nonhomologous end-joining repair, since repair using templates other than the sister, such as alleles on homologous chromosomes or repetitive elements on different chromosomes, could be mutagenic, resulting in loss of heterozygosity or chromosomal translocations, respectively (2, 3). HDR may therefore be finely balanced with nonhomologous repair to maintain genomic integrity, such that when genes involved in one pathway of DSB repair are disrupted, genomic integrity is perturbed.

RAD51 protein performs strand-exchange between homologous DNA molecules and so is postulated to be essential for homologous recombination reactions, and BRCA1 and BRCA2, products of the hereditary breast cancer genes, co-localize with RAD51 to nuclear foci following DNA damage in mitotic cells (4, 5). Both human and rodent cell lines that are deficient in these proteins are sensitive to DNA damaging agents that create DSBs, implicating these proteins in DSB repair (6). Our goal has been to determine if mutation of BRCA1 or BRCA2 affects HDR, therefore, making the proteins genomic caretakers.

BODY

Statement of work:

Task: To analyze gene targeting and the homologous repair of induced DSBs in Brca2-deficient ES cells.

- Quantitate gene targeting efficiencies in Brca2-deficient and parental ES cells using pimhyg targeting constructs; analyze the fidelity of the gene targeting event by Southern and PCR analysis
- Create additional recombination substrates cloned within the pimhyg targeting construct to test the role of BRCA1 in the recombinational repair of additional I-*Sce* I repair templates
- Quantitate homologous repair of DSBs in Brca2 mutant cells by adding the I-*Sce* I endonuclease

The *Brca2*$^{lex1/lex2}$ and control ES cell lines (7) were tested for gene targeting proficiency at the *pim1* locus on chromosome 17 (8, 9). The previously published design was modified in our to create an additional recombination substrate cloned within the pimhyg targeting vector (Figure 1A) that will be described in detail below. This new substrate allows a direct comparison of DSB-promoted gene conversion in Brca1- and Brca2-deficient cells.

Figure 1 Gene targeting vector and results of Brca2 DR-GFP gene conversion assays

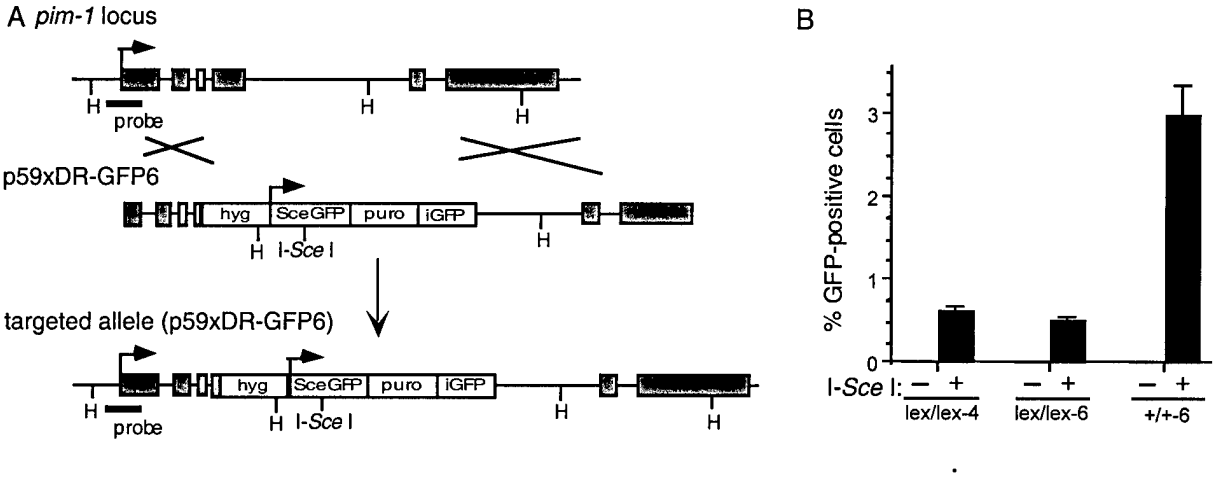

The pimhyg gene targeting vectors contain a promoterless hygromycin resistance (*hyg*^{R}) gene cloned in frame with *pim1* coding sequences. The *hyg* gene is expressed when the vector correctly gene targets at the *pim1* locus or when a fortuitous nonhomologous integration occurs adjacent to promoter sequences. The pimhyg targeting vectors (p59DRGFP4 and p59DRGFP6) were electroporated into both cell lines and *hyg*^{R}colonies were selected. Southern analysis demonstrated that gene targeted *hyg*^{R} *Brca2*$^{lex1/lex2}$ clones were derived but at a lower efficiency the wild-type ES cells (Table 1). The decrease was about 2-fold.

Table 1

Cell line	pim1 Targeting Efficiency
ES (wild-type)	139 targeted /144 total clones
Brca2$^{lex1/lex2}$	64 targeted / 121 total clones

Repair of chromosomal DSBs by intrachromosomal gene conversion was next investigated in the Brca2-deficient and control ES cell lines. During the process of gene targeting, a gene conversion substrate called DR-GFP (10) was integrated at the *pim1* locus, since this substrate had been previously cloned into the pimhyg targeting vector (Figure 1A). DR-GFP is composed of two differentially mutated green fluorescent protein (GFP) genes. GFP serves as marker gene since a GFP+ gene indicates that a gene conversion event occurred. The two GFP genes are oriented as direct repeats and separated by a drug selection gene for puromycin resistance (10). The SceGFP gene is mutated to contain the recognition site for I-*Sce* I, a rare-cutting endonuclease, so that DSBs can be induced in the substrate *in vivo*. The I-*Sce* I site was introduced in the GFP gene at a *Bcg* I restriction site by substituting 11 base pairs (bp) of wild-type GFP sequences with those of the I-*Sce* I site. These substituted bp also supply two in-frame stop-codons, which terminate translation and inactivate the protein. Downstream of the SceGFP gene is a 0.8 kb internal GFP fragment termed iGFP, and the two homologous mutated GFP genes are separated by 3.7 kb.

Figure 2 Analysis of homologous repair in GFP positive cells

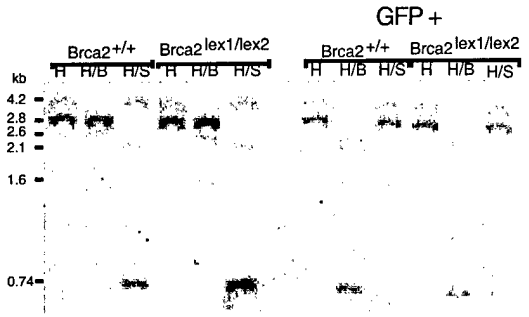

Gene conversion initiated by a DSB at the I-*Sce* I site restores an intact GFP gene whose expression is detected by cellular fluorescence. Several gene targeted cell clones were analyzed for each cell line and for two orientations of the DR-GFP substrate. Cells were electroporated with an I-*Sce* I expression vector or control DNAs and then analyzed for fluorescence on a flow cytometer. Results are shown in Figure1B. The wild-type cell clones had average gene conversion frequencies of approximately 3%, whereas the *Brca2*$^{lex1/lex2}$ cell clones had average frequencies of about 0.5% irrespective of the orientation of the DR-GFP substrate. Thus, DSB-promoted homologous repair is decreased with *Brca2* mutation. The GFP positive cells were sorted from both cell lines and shown to have undergone the expected gene conversion event

(Figure 2). In these sorted cells the I-*Sce* I site was converted to a *Bcg* I site (see also Figure 1A).

These results are consistent with our initial hypothesis that BRCA2 plays a key role in recombinational repair of chromosomal breaks. Gene conversion is a very precise form of DSB repair and is not mutagenic when it occurs between sister-chromatids which we have previously demonstrated is assayed by direct repeat recombination, as in our gene conversion substrate DR-GFP. Therefore, *BRCA2* mutation alters an important DNA repair pathway.

Task: To analyze gene targeting and the recombinational repair of induced DSBs in BRCA1-deficient ES cells and complemented mutant cells.

- Quantitate gene targeting efficiencies in BRCA1-deficient, complemented, and parental ES cells using pimhyg targeting constructs; analyze the fidelity of the gene targeting event by Southern and PCR analysis
- Quantitate homologous repair of DSBs in these cells by adding the I-*Sce* I endonuclease

The *Brca1*$^{-/-}$ 236.44, transgene complemented, and control *Brca1*$^{+/-}$ 310.7 cell lines (11) were tested for gene targeting proficiency at the *pim1* locus on chromosome 17, using the pimhyg targeting design (Fig. 1). The pimhyg targeting vector was electroporated into cell lines and *hyg/pur*^{R}colonies were selected. Southern analysis demonstrated that most of the *Brca1*$^{-/-}$ clones were derived from random integration of the targeting vectors, with only 6% of clones derived from gene targeting (Table 2). By contrast, efficient gene targeting was observed in the *Brca1*$^{+/-}$ and *Brca1*$^{+/+}$ cell lines, with greater than 90% of the clones correctly targeted. Transgene complementation led to an intermediate phenotype, such that almost 62% were correctly targeted.

Table 2 Gene targeting efficiency at the *pim1* locus

Genotype	Gene targeting efficiency (no. targeted clones/total analyzed)	FD
Brca1$^{+/+}$	96.7% (58/60)	-
Brca1$^{+/-}$	94.1% (48/51)	1.0
Brca1$^{-/-}$	5.9% (2/34)	16.4
Brca1$^{-/-,Tg+}$	61.9% (52/84)	1.6

Cells were electroporated with linearized p59xDR-GFP6 and selected in hygromycin (110 μg/ml) and puromycin (1μg/ml). Tg, wild-type *Brca1* transgene. FD, fold decrease

We next investigated the Brca1-deficient and control ES cell lines for the repair of chromosomal DSBs by intrachromosomal gene conversion (Fig. 3). The $Brca1^{+/+}$ and $Brca1^{+/-}$ showed identical results; however, the $Brca1^{-/-}$ cells had a 5-fold reduction in gene conversion. This reduction was partially, but not completely suppressed by transgene complementation.

Figure 3 Results of Brca1 DR-GFP gene conversion assays

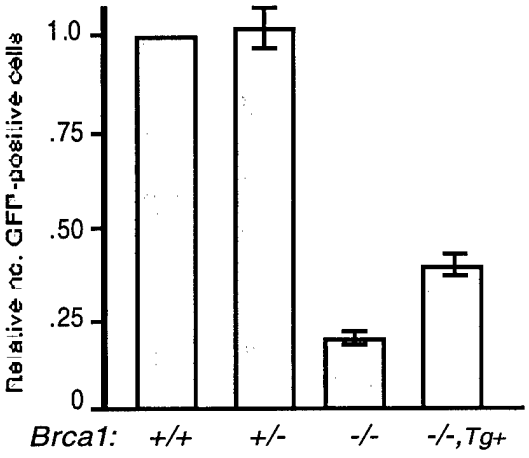

Task: To determine the reason why complementation of the Brca1-deficient cells did not restore gene targeting and homologous repair.

- Correct one of the mutant Brca1 alleles
- Measure sensitivity of corrected cells to a DNA damaging agent

The incomplete restoration of homologous recombination in the *Brca1* transgene-complemented cell lines could be due to inadequate expression of *Brca1* or even undetected alterations in the *Brca1* transgene upon integration. It is also formally possible that genomic changes occurred in the $Brca1^{-/-}$ cell line that contributed to the observed repair defects. This was a particular concern given the dramatic chromosomal instability observed in MEFs harboring a similar *Brca1* mutation.

To better address the dependence of the repair defects on Brca1-deficiency, a gene-targeting fragment was constructed to correct the exon 11 deletion mutation in the *Brca1*$^{-/-}$ 236.44 cell line. The *Brca1* alleles in this line are disrupted by replacement of the 3' end of intron 10 and 1.5 kb from the 5' end of exon 11 with *neo* and hypoxanthine phosphoribosyl transferase *(hprt)* selectable marker genes. To correct one of these alleles, a targeting fragment was constructed in which the *hyg*^{R} gene was inserted into intron 9 of wild-type murine *Brca1* genomic sequences. Gene targeting of this fragment at either *Brca1* allele would therefore restore an intact exon 11, giving rise to a *Brca1*$^{+gt}$ allele. In wild-type ES cells, we found a high targeting efficiency, such that 75 to 90% of the *hyg*^{R} clones had homologously integrated this fragment at the *Brca1* locus. Thus, even though gene targeting is substantially reduced in the *Brca1*$^{-/-}$ cell line, the high targeting efficiency of this fragment suggested that we would be able to obtain homologous integrations with sufficient screening of *hyg*^{R} clones.

As the *Brca1*$^{-/-}$ cell lines with the integrated DR-GFP substrate were already *hyg*^{R}, the parental *Brca1*$^{-/-}$ 236.44 cell line was electroporated with the targeting fragment. Two of 159 *hyg*^{R} clones had undergone a correction of the *neo* allele. Whereas most of the clones gave two distinct fragments for the *hprt* and *neo* alleles (11.6 and 5.9 kb, respectively), as in the parental *Brca1*$^{-/-}$ cell line, in the two targeted clones, E4 and H7, the *neo* fragment was replaced with a fragment expected for a targeted *Brca1*$^{+gt}$ *hyg* allele (11.3 kb; data not shown).

Because insertions into the intron of a gene can sometimes disrupt its expression, we determined if *Brca1* mRNA was restored in the targeted clones by performing Northern blot analysis. *Brca1*$^{+/-}$ cells were found to express the wild-type 7.2 kb *Brca1* mRNA, which was not present in the *Brca1*$^{-/-}$ cells (data not shown). Rather a 3.9 kb transcript is seen in the mutant

cells that results from the exon 10-12 splice. In the E4 and H7 *Brca1*$^{-/+gt}$ clones, the 7.2 kb mRNA was observed, indicating restoration of *Brca1* expression. Quantitation of *Brca1* expression in these clones indicated that mRNA levels were similar to the *Brca1*$^{+/-}$ cells.

To determine if restoration of *Brca1* expression in the *Brca1*$^{-/+gt}$ cells led to normal levels of mitomycin-C resistance, the E4 and H7 clones were analyzed in clonogenic survival assays, together with the control cells. Unlike the transgene complemented lines, restoration was nearly complete in both of the *Brca1*$^{-/+gt}$ clones, as compared to both wild-type and heterozygote *Brca1* cells (Figure 4). This functional restoration suggests that the HDR defects observed in the *Brca1*$^{-/-}$ 236.44 cell line is due specifically to the *Brca1* mutation, rather than other genetic alterations.

Figure 4. Correction of a Brca1 mutant allele restores mitomycin C resistance

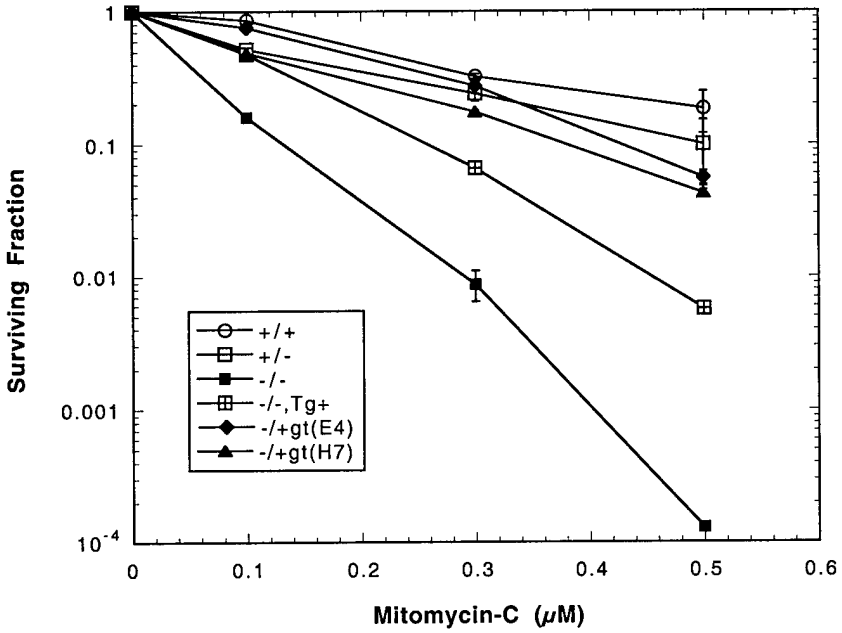

Unpublished results

Task: Express a BRC repeat to specifically disrupt the BRCA2 interaction with Rad51 during induced I-*Sce* I chromosomal cleavage for the analysis of DSB repair, including LOH and chromosomal translocations

- create dominant-negative expression plasmids for the wild-type (and, for a control, mutant) open reading frames of BRCA2 for functional inhibition of BRCA2/Rad51 protein interactions

We have created a dominant-negative expression plasmid for disrupting the BRCA2-Rad51 interaction by expressing a BRC repeat from BRCA2 which has been shown to interact with Rad51 (12). The BRC repeat 3 (or BRC3), a small peptide of 70 amino acids, is expressed using a chicken ß-actin promoter. We have expressed this peptide in a wild-type ES cell line containing the DR-GFP vector and found that the DSB by gene conversion is consistently reduced by expression of this peptide. Thus this interaction appears to be important for Rad51 activity. We are currently expressing this peptide in cell lines containing allelic recombination substrates to examine LOH (2) and substrates to measure translocations (3) to see if chromosomal rearrangements are altered.

KEY RESEARCH ACCOMPLISHMENTS

- Created a marker gene conversion recombination substrate cloned within the pimhyg targeting construct to test the role of Brca1 and Brca2 in the recombinational repair of an I-*Sce* I-induced chromosomal DSB
- Quantitated gene targeting efficiencies in Brca2-deficient and parental ES cells using the pimhyg targeting constructs containing the gene conversion substrate
- Quantitated DSB-induced gene conversion in Brca2-deficient and parental ES cells using pimhyg targeting constructs
- Quantitated gene targeting efficiencies in Brca1-deficient, complemented, and parental ES cells using the pimhyg targeting constructs containing the marker gene conversion substrate
- Quantitated DSB-induced gene conversion in Brca1-deficient, complemented, and parental ES cells using pimhyg targeting constructs
- Corrected a Brca1 mutant allele in a Brca1-deficient ES cell line
- Restored mitomycin C resistance in the Brca1 mutant line

- Quantitated DSB-induced gene conversion in wild-type ES cells expressing a BRC repeat from BRCA2

REPORTABLE OUTCOMES

- Development of ES cell lines deficient in Brca1 and Brca2 which contain gene conversion recombination reporter marker substrates at the *pim1* locus

- Brca1 corrected mouse ES cell line

- Development of dominant negative BRC repeat peptide expression vector for use in DR-GFP recombination studies

- Manuscripts:

Moynahan, M. E., Pierce, A. J., and Jasin, M. (2001). BRCA2 Is required for homology-directed repair of chromosomal breaks. Mol Cell *7*, 263-272.

Moynahan, M. E., Cui, T. X., and Jasin, M. (2001). Homology-directed DNA repair, mitomycin-C resistance, and chromosome stability is restored with correction of a *Brca1* mutation. Cancer Res *61*, 4842-4850.

-Abstracts:

FASEB Genetic Recombination July, 2001 Snowmass, CO Homologous Recombination, Genomic Integrity, and Cancer; Mary Ellen Moynahan, Jeremy Stark, Roger Johnson, Ulrica Westermark, and Maria Jasin.

CSH Symposium May, 2000 CSH, NY Homology-directed repair as a safeguard of genome integrity in mammalian cells Mary Ellen Moynahan, Roger Johnson, Andrew Pierce, Tracy Cui, & Maria Jasin

-Grants applied for: NIH P01

CONCLUSIONS

Our results support the hypothesis that BRCA1 and BRCA2 play a role in homologous repair of chromosome breaks. These proteins, therefore, have a role in preserving genomic integrity, such that mutations would be expected to be tumor promoting as a result.

Personnel list – Drs. Maria Jasin, Mary Ellen Moynahan, Tracy Cui, Biao Wu, and Ms. Jin Oh

REFERENCES

1. R. D. Johnson, M. Jasin, *EMBO J.* **19,** 3398-3407 (2000).
2. M. E. Moynahan, M. Jasin, *Proc. Natl. Acad. Sci. USA* **94**, 8988-8993 (1997).
3. C. Richardson, M. Jasin, *Nature.* **405**, 697-700 (2000).
4. J. Chen, et al., *Mol. Cell* **2**, 317-28 (1998).
5. R. Scully, et al., *Cell* **88**, 265-75 (1997).
6. M. Jasin, in *DNA Damage and Repair* J. A. Nickoloff, M. F. Hoekstra, Eds. (Humana Press, Totowa, N.J., 2001), vol. III.
7. M. Morimatsu, et al. *Cancer Res.* **58,** 3441-3447 (1998).
8. H. te Riele, E. R. Maandag, A. Clarke, M. Hooper, A. Berns, *Nature* **348**, 649-651 (1990).
9. M. E. Moynahan, J. W. Chiu, B. H. Koller, M. Jasin, *Molecular Cell* **4**, 511-518 (1999).
10. A. J. Pierce, R. D. Johnson, L. H. Thompson, M. Jasin, *Genes Dev.* **13**, 2633-2638 (1999).
11. L. C. Gowen, B. L. Johnson, A. M. Latour, K. K. Sulik, B. H. Koller, *Nat. Genet.* **12**, 191-194 (1996).
12. C.F. Chen, P. L. Chen, Q., Zhong,, Z. D. Sharp, and W. H. Lee, *J. Biol. Chem.* **274,** 32931-32935 (1999).

Molecular Cell, Vol. 7, 263–272, February, 2001, Copyright ©2001 by Cell Press

BRCA2 Is Required for Homology-Directed Repair of Chromosomal Breaks

Mary Ellen Moynahan,*† Andrew J. Pierce,† and Maria Jasin†‡
*Department of Medicine
†Cell Biology Program
Memorial Sloan-Kettering Cancer Center
New York, New York 10021

Summary

The BRCA2 tumor suppressor has been implicated in the maintenance of chromosomal stability through a function in DNA repair. In this report, we examine human and mouse cell lines containing different *BRCA2* mutations for their ability to repair chromosomal breaks by homologous recombination. Using the I-SceI endonuclease to introduce a double-strand break at a specific chromosomal locus, we find that BRCA2 mutant cell lines are recombination deficient, such that homology-directed repair is reduced 6- to >100-fold, depending on the cell line. Thus, BRCA2 is essential for efficient homology-directed repair, presumably in conjunction with the Rad51 recombinase. We propose that impaired homology-directed repair caused by BRCA2 deficiency leads to chromosomal instability and, possibly, tumorigenesis, through lack of repair or misrepair of DNA damage.

Introduction

Germline mutations in either of the breast cancer susceptibility genes *BRCA1* or *BRCA2* predispose to breast, ovarian, and other cancers (Rahman and Stratton, 1998). Inheritance of one defective allele of either gene is sufficient to confer cancer predisposition, but tumors from predisposed individuals consistently exhibit loss of heterozygosity, implying that the *BRCA1* and *BRCA2* gene products act as tumor suppressors. Both genes encode large nuclear proteins whose function in tumor suppression has been a matter of speculation, although roles in both DNA repair and transcription have been ascribed (Welcsh et al., 2000).

Common to BRCA1 and BRCA2 is a physical interaction with the mammalian Rad51 protein, a homolog of bacterial RecA that catalyzes strand exchange during homologous recombination (Cox, 1999). Both proteins colocalize with Rad51 to nuclear foci after DNA damage and at forming synaptonemal complexes early in meiotic prophase (Scully et al., 1997; Chen et al., 1998a). The interaction of BRCA2 with Rad51 is mediated by a series of internal BRC repeats (Wong et al., 1997; Chen et al., 1998b), with an additional Rad51-interacting domain described for mouse Brca2 at the extreme C terminus (Mizuta et al., 1997; Sharan et al., 1997). Consistent with a role for these proteins in DNA repair, BRCA1- and BRCA2-deficient mouse and human cells display chromosome instability and are sensitive to DNA-damaging agents, particularly those agents that cause DNA double-strand breaks (DSBs; Connor et al., 1997; Sharan et al., 1997; Chen et al., 1998b; Gowen et al., 1998; Patel et al., 1998; Shen et al., 1998; Abbott et al., 1999).

Homologous recombination is a conserved pathway for the repair of DSBs, with Rad51 postulated to play a central role (Cox, 1999; Pâques and Haber, 1999). In mammals, as in other organisms, homology-directed repair (HDR) of a DSB maintains genomic integrity through precise repair by gene conversion, using the sister chromatid as a repair template (Johnson and Jasin, 2000). Nonhomologous repair mechanisms also play a major role in the repair of DSBs in mammalian cells, although this type of repair is generally thought to be imprecise and potentially more mutagenic (Jeggo, 1998). BRCA1-deficient cells have recently been demonstrated to have impaired HDR of a chromosomal DSB, whereas nonhomologous repair was not diminished (Moynahan et al., 1999). A similar role for BRCA2 as a caretaker of genomic stability would suggest that BRCA2 inactivation could foster tumorigenesis by increasing the likelihood that cells would accrue mutations in genes that control cell division, death, or life span.

In this study, we sought to directly determine whether BRCA2 plays a role in homologous repair of DSBs by examining the repair of a DSB introduced into a defined site in the genome. We report that human and murine cells carrying different *BRCA2* mutations have a diminished capacity to repair a chromosomal DSB by gene conversion. These findings establish a biological function for BRCA2 that is relevant to carcinogenesis.

Results

BRCA2-Deficient CAPAN-1 Cells Are Defective in HDR

The human pancreatic adenocarcinoma cell line, CAPAN-1, carries a 6174delT mutation on one allele of *BRCA2* with loss of the wild-type *BRCA2* allele (Goggins et al., 1996). This frameshift mutation, which is frequent in families with hereditary breast and ovarian cancer, leads to a truncation after amino acid 1981 within BRC repeat 7 (Figure 1A). Consistent with this, the CAPAN-1 cell line has been demonstrated to express a truncated BRCA2 protein (Marmorstein et al., 1998; Su et al., 1998).

This cell line was reported to be hypersensitive to genotoxic agents specifically capable of producing DNA DSBs (Abbott et al., 1998; Chen et al., 1998b). To test whether the hypersensitivity is due to impaired HDR of chromosomal DSBs, we introduced a recombination repair substrate into the CAPAN-1 genome (Figure 2). The repair substrate incorporates a direct repeat green fluorescent protein (DR-GFP) reporter, and assays noncrossover gene conversion events (Pierce et al., 1999). DR-GFP is composed of two differentially mutated green fluorescent protein (GFP) genes (Figure 2A). The *SceGFP* gene is a mutated GFP gene that contains the 18 bp recognition site for the rare cutting I-SceI endonuclease,

‡To whom correspondence should be addressed (e-mail: m-jasin@ski.mskcc.org).

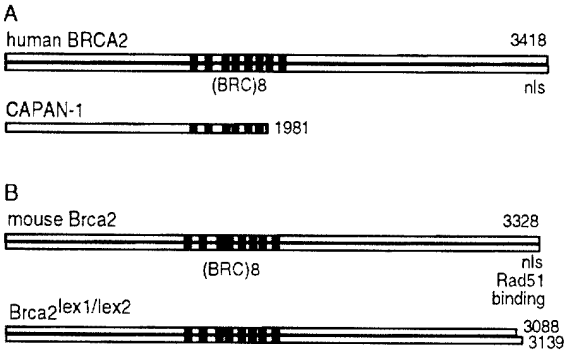

Figure 1. Schematic of Wild-Type and Mutant BRCA2 Proteins

(A) Human BRCA2 protein is 3418 amino acids long. Notable structural motifs include a centrally located region of eight BRC repeats (black bars) that interacts with Rad51 and a C-terminal nuclear localization signal (nls). In the CAPAN-1 pancreatic cancer cell line, one *BRCA2* allele contains a 6174delT mutation and the other allele is lost. The mutant *BRCA2* allele encodes a truncated protein of 2002 amino acids, including 1981 BRCA2 amino acids and 21 amino acids that are generated by the frameshift. The truncation of BRCA2 sequences at amino acid 1981 occurs within BRC repeat 7.

(B) The murine Brca2 protein is 3328 amino acids long, and is 59% identical to human BRCA2, although specific regions are highly conserved (Sharan and Bradley, 1997). Conserved regions include the centrally located BRC repeats and the nls (amino acids 3189–3238). An additional Rad51-interacting domain was identified at the same region in the C terminus of the murine protein as the nls (amino acids 3196–3232). *Brca2*$^{lex1/lex2}$ ES cells harbor two different alleles, both of which encode truncated Brca2 proteins deleted for the C-terminal Rad51-interacting domain and the conserved nls identified by sequence homology.

and as a result will undergo a DSB when I-SceI is expressed in vivo. The I-SceI site was incorporated at a BcgI restriction site by substituting 11 bp of wild-type GFP sequences with those of the I-SceI site. These substituted base pairs also introduce two in-frame stop codons. Downstream of *SceGFP* is an 812 bp internal GFP fragment *(iGFP)* that can be used to correct the mutation in the *SceGFP* gene to result in a *GFP+* gene. Molecular analysis has previously confirmed that GFP-positive cells following I-SceI expression are derived from a noncrossover gene conversion within the DR-GFP substrate (Pierce et al., 1999). By contrast, deletional recombinational events give rise to a 3′-truncated GFP gene that has been shown to be nonfunctional for GFP expression (Pierce et al., 1999). The two GFP genes are separated by a puromycin resistance gene that is used to select for integration of the DR-GFP substrate into the genome of cells.

The DR-GFP substrate was electroporated into CAPAN-1 cells, and clones that had randomly integrated the substrate into the genome were selected with puromycin. Six independently isolated clones were identified by Southern analysis to have undergone integration of an intact, single copy DR-GFP substrate (+, Figure 2B; data not shown). Multiple digests were performed to confirm that the integrated recombination substrate was a single copy, and that no gross changes in the integrity of the reporter substrate had occurred prior to integration (data not shown).

To detect HDR of an induced chromosomal DSB, the I-SceI expression vector pCBASce was transiently transfected into five of the CAPAN-1 DR-GFP clones, and flow cytometry was used to quantify GFP-positive cells (Figure 2C). Due to the slow growth characteristics of CAPAN-1 cells, flow cytometry was performed at different time points to determine the time after transfection for maximal detection of GFP-positive cells. A few GFP-positive cells (0.0086%) were detected maximally 5 days after transfection of pCBASce (Figure 2C; Table 1; data not shown). No GFP-positive cells (or only extremely rare ones) were detected following transfection with negative control DNA, indicating that spontaneous intrachromosomal gene conversion was rare, and that the few GFP-positive cells from I-SceI expression were from DSB-induced recombination. Combining data from the five CAPAN-1 clones, the I-SceI-generated DSB induced HDR approximately 20-fold. This induction of HDR is significantly less than we have typically found in other cell lines with this recombination reporter (Pierce et al., 1999). We attempted to complement the CAPAN-1 cell line by expressing full-length BRCA2 from a cDNA expression vector (Marmorstein et al., 1998). However, we have thus far been unable to detect appreciable expression levels, presumably due to difficulties in expressing this large protein.

To verify that the low frequency of HDR is not due to poor transfection efficiency, the CAPAN-1 clones were also electroporated with the pNZE-CAG vector, which expresses wild-type GFP protein from the same control elements as I-SceI in the pCBASce vector. Maximal GFP expression was detected 3 days after electroporation at a frequency of 12% of the electroporated cells (data not shown), and then declined 5 days after transfection to an average of 4% (Table 1). We can surmise, therefore, that HDR is occurring in approximately 1 per 1400 cells successfully transfected with the I-SceI expression vector, based on a 12% transfection efficiency and an average frequency of recombination of 0.0086%.

We have typically found that a DSB introduced into the genome of rodent cells within the DR-GFP substrate leads to as much as a three order-of-magnitude induction of homologous recombination (Pierce et al., 1999). More recently, we have tested a variety of immortalized human cell lines for HDR and found a similarly large induction of gene conversion, such that recombinants are at least 5% to 10% of the electroporated cells (our unpublished data). With this large induction, recombination is estimated to occur in roughly 1 in 10 cells successfully transfected with the I-SceI expression vector. Thus, the CAPAN-1 cells have more than a 100-fold reduction in homologous repair as compared with other cell lines.

Gene Targeting Is Reduced in *Brca2*$^{lex1/lex2}$ Mouse ES Cells

Due to difficulties in complementing the BRCA2 defect in CAPAN-1 cells as well as the inherent questions raised when analyzing the functional role of gene products in tumor-derived cell lines, we examined the role of BRCA2 in a more genetically defined system. For this, we used murine embryonic stem (ES) cells containing hypomorphic *Brca2* alleles. In addition to the conserved internal BRC repeats, a second Rad51-interacting domain was identified at the C terminus of the mouse Brca2 protein

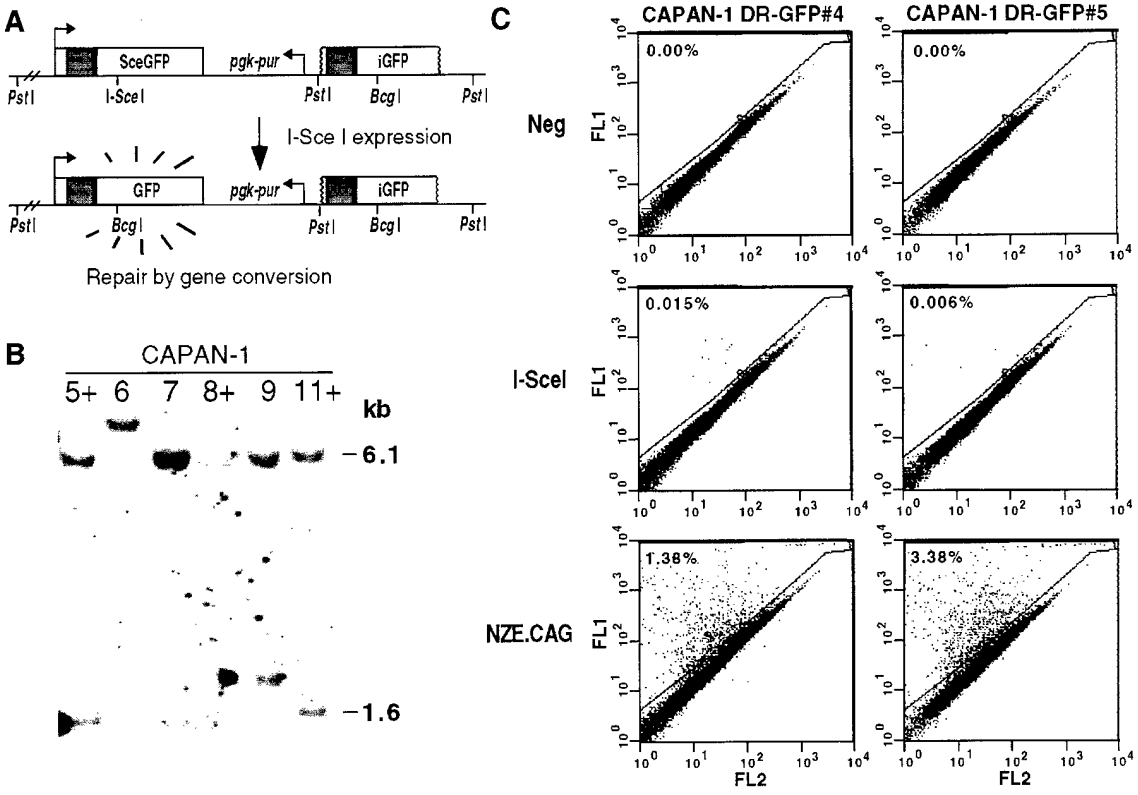

Figure 2. HDR of an Induced DSB in CAPAN-1 Cells Is Defective

(A) The recombination repair substrate DR-GFP is composed of two differentially mutated GFP genes, *SceGFP* and *iGFP.* When I-SceI endonuclease is expressed in cells containing the DR-GFP substrate in their genome, a DSB will be introduced at the I-SceI site in the *SceGFP* gene. Repair of the DSB by a noncrossover gene conversion with the downstream *iGFP* gene results in reconstitution of a functional GFP gene, involving loss of the I-SceI site and gain of the BcgI site. Because the I-SceI site mutation in the *SceGFP* gene entails 11 bp changes including the introduction of two stop codons, homologous recombination between *SceGFP* and *iGFP* is necessary to restore a functional GFP gene (Pierce et al., 1999). The *SceGFP* gene is expressed from the chicken β-actin promoter with cytomegalovirus enhancer sequences. The shaded regions indicate that *SceGFP* and the corrected GFP genes encode an EGFP protein (mutated or wild-type, respectively) fused to a nuclear localization signal (light shading) and zinc finger domain (dark shading) to aid in nuclear retention of the protein (Pierce et al., 1999).

(B) Southern blot analysis of CAPAN-1 clones derived from electroporation of the DR-GFP substrate. Genomic DNA from puromycin-resistant clones was digested with PstI and probed with a radiolabeled GFP fragment. Intact integration of the DR-GFP substrate gives 6.1 and 1.6 kb fragments containing the *SceGFP* and *iGFP* genes, respectively. CAPAN-1 clones 5, 8, and 11 contain the expected fragments from PstI and other restriction analyses, as do clones 4 and 23 (data not shown).

(C) Representative flow cytometric analyses of CAPAN-1 DR-GFP clones to detect cellular green fluorescence following DSB induction. Panels depict clones 4 and 5 following transfection with negative control DNA (top panels), the I-SceI expression vector pCBASce (middle panels), and the GFP expression vector pNZE-CAG (bottom panels). Two-color fluorescence analysis was performed, with the percentage of green fluorescent cells above the diagonal indicated. In each panel, 50,000 cells were analyzed. Flow cytometry shown here was performed 5 days after transfection. FL1, green fluorescence; FL2, orange fluorescence.

by two-hybrid analysis (Mizuta et al., 1997; Sharan et al., 1997). Consecutive gene targeting with two different vectors was performed in ES cells to create a cell line in which both alleles are deleted for this interacting domain, which is encoded by exon 27 (Morimatsu et al., 1998). In the *lex1* allele, only sequences encoded by exon 27 of *Brca2* were deleted, whereas in the *lex2* allele, sequences from exon 27 and part of exon 26 of *Brca2* were deleted (Figure 1B). Although the internal BRC repeats are not perturbed in the $Brca2^{lex}$ alleles, $Brca2^{lex1/lex2}$ cells are hypersensitive to ionizing radiation, indicating a functional significance for the extreme C terminus of the protein (Morimatsu et al., 1998).

We first performed gene targeting assays with the $Brca2^{lex1/lex2}$ ES cells to determine their ability to homologously integrate transfected DNA. Although the precise relationship between gene targeting and HDR has not been established, cell lines with defects in HDR have also been shown to have gene-targeting defects (Essers et al., 1997; Moynahan et al., 1999; Dronkert et al., 2000). To analyze gene targeting, we constructed a vector that incorporates the DR-GFP recombination substrate. In this way, HDR at a defined genetic locus could subsequently be assayed in the gene-targeted clones. The DR-GFP substrate was subcloned in both orientations into a gene-targeting vector for the *pim1* locus on chromosome 17 (te Riele et al., 1990), creating the p59xDR-GFP vectors (see Figure 3A). In these vectors, the selectable hygromycin resistance gene (hyg^R)–coding sequences are fused in-frame to *pim1*-coding sequences, such that

Table 1. CAPAN-1 Cells Exhibit Low Levels of Homologous DSB Repair

CAPAN-1 Clone	Number of GFP-Positive Cells		
	Negative	pCBASce	pNZE-CAG
#4	$<1 \times 10^{-5}$	1.5×10^{-4}	2.9×10^{-2}
#5	$<1 \times 10^{-5}$	0.6×10^{-4}	4.8×10^{-2}
#8	$<1 \times 10^{-5}$	0.3×10^{-4}	3.5×10^{-2}
#11	1×10^{-5}	1.0×10^{-4}	ND
#23	1×10^{-5}	0.9×10^{-4}	ND
All clones	0.4×10^{-5} ($\pm 0.5 \times 10^{-5}$)	0.86×10^{-4} ($\pm 0.45 \times 10^{-4}$)	3.7×10^{-2} ($\pm 1.0 \times 10^{-2}$)

CAPAN-1 DR-GFP cells were transfected with negative DNA, pCBASce, and pNZE-CAG. FACS analysis was performed at 5 days posttransfection. Numbers for each clone are from the average of two or three experiments per cell clone, with 50,000 cells analyzed per experiment. GFP-positive cells after pCBASce transfection are presumably derived from the recombination of the GFP gene in the chromosome, and reach a maximum level at 5 days posttransfection. GFP-positive cells after pNZE-CAG transfection are derived from the transient expression of the plasmid GFP gene, and reach a maximum level at 3 days posttransfection. (The number of transiently GFP-positive cells at 3 days is approximately 3-fold higher than at 5 days.)
ND, not determined.

cellular hygromycin resistance is dependent on either homologous targeting to the *pim1* locus or a fortuitous nonhomologous integration adjacent to random promoter sequences.

Linearized p59xDR-GFP6- and p59xDR-GFP4-targeting vectors, which contain DR-GFP in the forward (Figure 3A) or reverse orientation (not shown), respectively, relative to the *pim1* locus, were electroporated into *Brca2*$^{+/+}$ and *Brca2*$^{lex1/lex2}$ ES cells, and *hyg*^{R} colonies were selected. Genomic DNA from individual *hyg*^{R} clones was examined by Southern blotting to determine which clones had undergone gene targeting (Figure 3B). Efficient gene targeting was observed with both targeting vectors in the wild-type ES cells, with 97% of *hyg*^{R} clones correctly targeted (139 targeted clones/144 total). The remaining clones were derived from fortuitous random integrations of the targeting vectors in which the *hyg* gene could be expressed. Homologous integrations were also detected in the *Brca2*$^{lex1/lex2}$ ES cells (64 targeted clones/121 total), but at an approximately 1.8-fold lower frequency. This diminished ability to gene target is suggestive of a homologous recombination defect in cells that are mutated for the *Brca2* gene.

Impaired HDR of a Chromosomal DSB by Gene Conversion in *Brca2*-Deficient ES Cells

Homologous integration of the DR-GFP substrate at the *pim1* locus allows us to examine the ability of cells to repair a DSB by gene conversion at a specific chromosome site. To analyze HDR in the ES cell lines, several of the targeted *Brca2*$^{+/+}$ and *Brca2*$^{lex1/lex2}$ clones were transiently transfected with the I-SceI expression vector (pCBASce), the GFP expression vector (pCAG-NZE), or a negative control DNA. Electroporated cells were typically examined 48 hr later by flow cytometry. Results from one set of experiments are shown in Figure 4A. GFP-positive cells were undetected or rarely detected (<0.01%) in either the wild-type or *Brca2*$^{lex1/lex2}$ clones

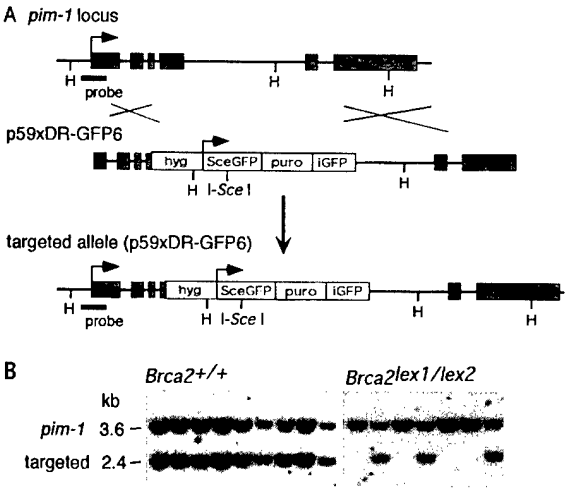

Figure 3. ES Cells with a *Brca2* Exon 27 Deletion Have Reduced Gene Targeting

(A) The *pim1* genomic locus and the p59xDR-GFP6 vector gene targeted to the *pim1* locus. Clones that are gene targeted at *pim1* are efficiently selected in hygromycin, since the *hyg*^{R} gene is promoterless in the targeting vector, but is expressed from the *pim1* promoter upon homologous integration. In p59xDR-GFP6, *SceGFP* and *iGFP* are in the same orientation as the *pim1*- and *hyg*-coding sequences. Not shown is the p59xDR-GFP4 vector, in which *SceGFP* and *iGFP* are in the opposite orientation, due to insertion of the entire DR-GFP substrate in the reverse direction into the p59x *pim*-targeting vector. H, HincII sites.

(B) Southern blot analysis of *hyg*^{R} clones derived from *Brca2*$^{+/+}$ and *Brca2*$^{lex1/lex2}$ ES cells transfected with a p59xDR-GFP-targeting vector. DNA from individually expanded clones was digested with HincII and hybridized with the *pim1* probe shown in (A).

transfected with the negative control DNA, indicating that spontaneous intrachromosomal gene conversion is rare. Following transfection with pCBASce, GFP-positive cells were readily detected in the *Brca2*$^{+/+}$ cells. The percentage of GFP-positive cells increased from 24 to 40 hr, where it then remained stable at approximately 3% of the electroporated cells.

In the *Brca2*$^{lex1/lex2}$ clones, recombination was also induced by I-SceI expression; however, the number of recombinants was lower relative to the *Brca2*$^{+/+}$ clones, at approximately 0.5% to 0.6% in this experiment (Figure 4A). A similar reduction in the recovery of recombinants was found for both orientations of the DR-GFP substrate. Over several experiments, the average reduction in recombination for the *Brca2*$^{lex1/lex2}$ clones, as compared with the *Brca2*$^{+/+}$ clones, was 5- to 6-fold. In control transfections of the GFP expression vector, equal numbers of GFP-positive cells were observed for both cell lines (data not shown), indicating that transfection efficiency is not compromised in the *Brca2*$^{lex1/lex2}$ cell lines.

The DR-GFP repair substrate was specifically designed to detect DSB repair by gene conversion. To confirm that GFP expression in cells was dependent on gene conversion, physical analysis was performed on the repair substrate in GFP-positive cells. *Brca2*$^{+/+}$ and *Brca2*$^{lex1/lex2}$ cells were transiently transfected with the I-SceI expression vector and then sorted by flow cytometry into GFP-positive and GFP-negative populations.

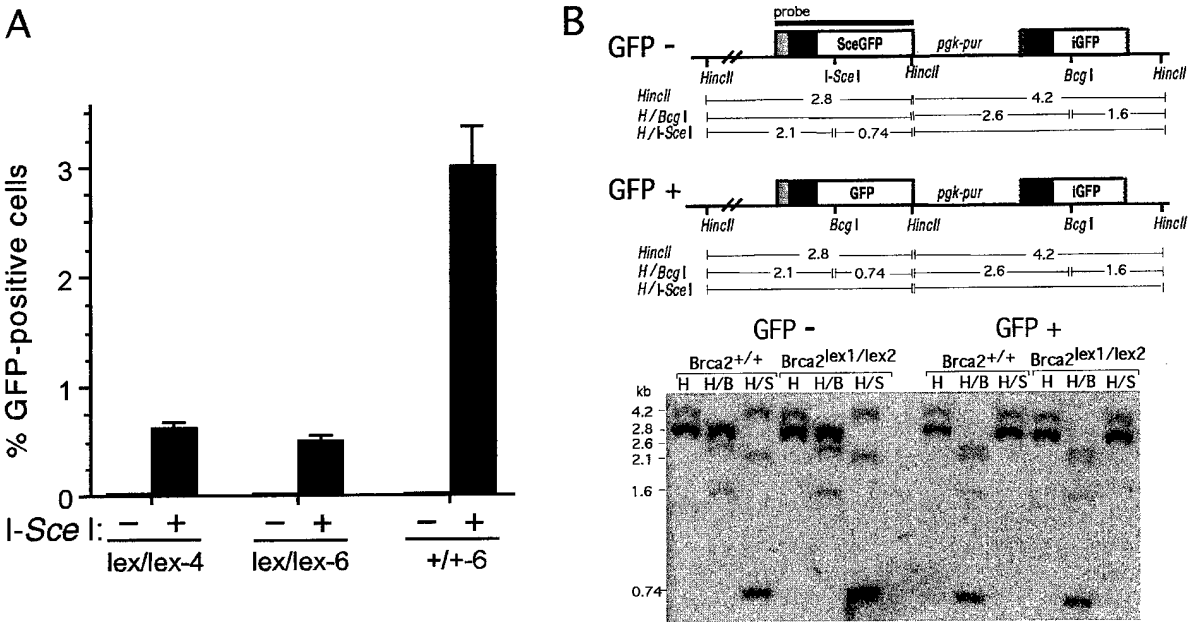

Figure 4. ES Cells with a *Brca2* Exon 27 Deletion Have Reduced HDR of DSBs

(A) Gene conversion within the DR-GFP substrate as deduced from the percentage of GFP-positive cells. Results from targeted $Brca2^{lex1/lex2}$ and $Brca2^{+/+}$ ES cell lines are shown from a representative experiment. Bars not detectable above the x axis depict the infrequent occurrence of GFP-positive cells after transfection with negative control DNA, whereas the visible black bars depict the percent GFP-positive cells following transfection of the I-SceI expression vector. I-SceI expression strongly induces the number of GFP-positive $Brca2^{+/+}$ cells, indicating robust DSB repair by gene conversion; however, $Brca2^{lex1/lex2}$ cells have 5- to 6-fold fewer GFP-positive cells, indicating impaired HDR of a DSB by gene conversion. In this analysis, at least seven independent clones from each mutant genotype were analyzed. lex/lex-4 indicates $Brca2^{lex1/lex2}$ cells targeted with the p59xDR-GFP4 vector; lex/lex-6 and +/+-6 indicate $Brca2^{lex1/lex2}$ and wild-type cells, respectively, targeted with the p59xDR-GFP6 vector. Error bars indicate the SEM.

(B) Physical confirmation of HDR of the I-SceI-induced DSB. After DSB induction, $Brca2^{+/+}$ and $Brca2^{lex1/lex2}$ cells were sorted based on GFP expression, and genomic DNA extracted from each of the sorted pools was analyzed by Southern blotting. Cells that do not express GFP after I-SceI expression (GFP−) retain the I-SceI site in the DR-GFP substrate. By contrast, cells that express GFP after I-SceI expression (GFP+) have repaired the I-SceI-induced DSB by gene conversion with the downstream *iGFP* gene fragment to restore the BcgI site. (Note: As this is a population analysis, cells present in the GFP-negative population at low frequency that have repaired the I-SceI site by other mechanisms would not be detected in this analysis.) H, HincII; B, BcgI; S, I-SceI.

After expansion, genomic DNA was extracted from each of the sorted pools and analyzed by Southern blotting. Whereas GPF-negative cells retained the I-SceI site in the DR-GFP substrate, GFP-positive cells had lost the site (Figure 4B). The I-SceI site in the GFP-positive cells was repaired with restoration of the BcgI site, providing conclusive evidence of DSB repair by gene conversion with the downstream *iGFP* gene fragment. This was apparent in GFP-positive populations derived from either the $Brca2^{+/+}$ or $Brca2^{lex1/lex2}$ cells, indicating that the GFP-positive cells in the $Brca2^{lex1/lex2}$ mutant were also derived by gene conversion rather than by a novel type of repair.

In Vivo Interaction of Brca2 with Rad51

The CAPAN-1 cell line, which harbors a BRCA2-truncating mutation within the BRC repeats (Figure 1A), rarely exhibited cellular green fluorescence following induction of a chromosome break, indicating a profound defect in HDR in these cell lines. However, the $Brca2^{lex1/lex2}$ cells, in which the truncating mutations are well removed from the BRC repeats, had a smaller reduction in HDR. Although it is difficult to directly compare the magnitude of a gene conversion defect in different cell types, it would seem probable that this difference is related to the extent of Brca2 truncation and the ability of the truncated proteins to be expressed and to interact with Rad51. A truncated BRCA2 protein has been demonstrated to be expressed in CAPAN-1 cells, although reports vary on the extent of expression (Marmorstein et al., 1998; Su et al., 1998). The truncated protein interacts with Rad51 by coimmunoprecipitation (Chen et al., 1998a; Marmorstein et al., 1998); however, the Rad51–BRCA2 complexes may be reduced (Marmorstein et al., 1998), and, significantly, the truncated protein is primarily detected in cytoplasmic extracts (Spain et al., 1999). Consistent with this, a nuclear localization signal was recently identified at the C terminus of the human BRCA2 protein, which is deleted in the truncated BRCA2 protein in CAPAN-1 cells (Spain et al., 1999; Yano et al., 2000).

Truncation of the mouse protein could likewise affect protein stability or localization. Although a nuclear localization signal for the mouse Brca2 protein has not been functionally determined, comparison of the mouse and human proteins shows significant sequence conservation in this region of the protein, which is encoded by exon 27 and therefore deleted in the $Brca2^{lex}$ alleles. To evaluate the stability and localization of the truncated mouse protein, Western blotting of extracts from the *Brca2* mutant cell line was performed with antibodies

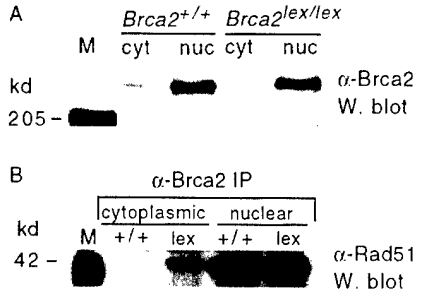

Figure 5. Brca2 Expression and Rad51–Brca2 Interaction in the *Brca2*$^{lex1/lex2}$ ES Cells

(A) Western blot analysis of cytoplasmic and nuclear extracts using an antibody directed against the BRCA2 protein. In both *Brca2*$^{+/+}$ and *Brca2*$^{lex1/lex2}$ ES cells, Brca2 is primarily nuclear. Immunoblotting was performed with the anti-BRCA2 Ab-2 antibody.

(B) Immunoprecipitation of nuclear and cytoplasmic extracts using an anti-BRCA2 antibody followed by Western blot analysis using an anti-Rad51 antibody as a probe. Nuclear coimmunoprecipitates are similar in both *Brca2*$^{+/+}$ and *Brca2*$^{lex1/lex2}$ ES cells, although *Brca2*$^{lex1/lex2}$ also shows a reproducible signal in the cytoplasm, albeit significantly lower than the nuclear signal. +/+, extracts from *Brca2*$^{+/+}$ cells; lex, extracts from *Brca2*$^{lex1/lex2}$ cells.

directed against Brca2. Fractionated extracts from the *Brca2*$^{lex1/lex2}$ ES cells demonstrated a robust signal that was predominantly localized to the nucleus (Figure 5A), despite deletion of the presumed nuclear localization signal. Thus, it is likely that there is another, as yet unidentified, motif in the mouse protein that can confer nuclear localization. In both wild-type and mutant cells, a small amount of the protein was apparent in the cytoplasmic extract.

Since Western blotting indicated that Brca2 protein was present in the *Brca2*$^{lex1/lex2}$ cells, further biochemical analysis was performed to determine whether the protein interacted with Rad51. Western blot analysis indicated that Rad51 levels were similar in *Brca2*$^{+/+}$ and *Brca2*$^{lex1/lex2}$ cells, and that it was distributed in both the nucleus and cytoplasm (data not shown), as has been found in human cells (Davies et al., 2001 [this issue of Molecular Cell]). Nuclear and cytoplasmic extracts derived from *Brca2*$^{+/+}$ and *Brca2*$^{lex1/lex2}$ cells were immunoprecipitated with the anti-Brca2 antibody and immunoblotted with an anti-Rad51 antibody (Figure 5B). Rad51–Brca2 interactions in the nucleus appeared unperturbed in the *Brca2*$^{lex1/lex2}$ cells, although some signal was also detected in the cytoplasm of these cells. Therefore, despite the loss of the C-terminal Rad51 interaction domain in the *Brca2*$^{lex1/lex2}$ cells, a deficiency in Rad51–Brca2 interaction is not apparent.

Discussion

These results directly demonstrate a role for BRCA2 in homologous recombination, specifically in efficient HDR of DNA damage. Impaired HDR of DSBs is observed in human cells that contain a common mutation in families at risk for breast cancer, as well as in a mouse cell line containing a targeted mutation. The magnitude of the defect in the human CAPAN-1 cells is >100-fold as compared with other human cell lines, whereas in the *Brca2*$^{lex1/lex2}$ ES cells, HDR is reduced 5- to 6-fold relative to wild-type ES cells. Thus, the severity of the defect was significantly greater in cells that express a highly truncated BRCA2 protein than in cells in which only the most C-terminal Rad51-interacting domain is perturbed. Gene targeting as assayed in the mouse cells was also reduced.

Although *BRCA1* and *BRCA2* show no homology, the two genes share several characteristics aside from a predisposition to breast and ovarian cancer when mutated. For example, disruptions of *Brca1* and *Brca2* in the mouse lead to early embryonic lethality, and both proteins colocalize to nuclear foci with Rad51. In addition to *BRCA2* mutant cell lines, we have previously examined homologous recombination in ES cells containing a *Brca1* hypomorphic allele (Moynahan et al., 1999). The magnitude of the HDR defect in the *Brca1* mutant cells was similar to that in the *Brca2*$^{lex1/lex2}$ cells. However, the gene-targeting defect was much more severe, approximately 20-fold in the *Brca1* mutant compared to less than 2-fold in the *Brca2* mutant. This suggests that, although these two proteins are both involved in homologous recombination, they have divergent contributions to different recombination pathways.

The HDR defect in the BRCA2-deficient cells is consistent with their hypersensitivity to ionizing radiation and other damaging agents that produce DSBs (Abbott et al., 1998; Chen et al., 1998b; Morimatsu et al., 1998). CAPAN-1 cells have also been found to be defective for ionizing radiation–induced foci of Rad51 (Rad51-IRIF), despite the ability of the truncated protein to interact with Rad51 (Marmorstein et al., 1998; Yuan et al., 1999). This is likely due to the cytoplasmic location of the BRCA2 and Rad51 proteins in these cells (Spain et al., 1999; Davies et al., 2001). The significance of Rad51-IRIF for DSB repair is unknown. However, in addition to BRCA2 mutants, three other cell lines that have defective Rad51-IRIF also have HDR defects. These cell lines are mutant for Brca1 (Moynahan et al., 1999; Bhattacharyya et al., 2000), Rad54 (Tan et al., 1999; Dronkert et al., 2000), and the Rad51-related protein XRCC3 (Bishop et al., 1998; Pierce et al., 1999). Although it is possible that BRCA2 and these other three proteins are each directly required for the physical assembly of Rad51 into nuclear foci, an alternative is that disruptions in HDR per se cause defects in Rad51-IRIF.

Null mutations of *Brca2*, like *Rad51* and *Brca1*, confer an early embryonic lethality in the mouse and an inability to recover viable cell lines (Hakem et al., 1996; Lim and Hasty, 1996; Liu et al., 1996; Tsuzuki et al., 1996; Ludwig et al., 1997; Sharan et al., 1997; Suzuki et al., 1997; Shen et al., 1998). *Brca2* hypomorphic alleles that allow animal and cell survival preserve at least a few BRC domains (Connor et al., 1997; Friedman et al., 1998; Morimatsu et al., 1998). Formally, it is possible that viability is unrelated to recombination; however, enough residual recombination activity may be preserved in these truncation mutants to permit survival. Consistent with this, our DSB assay detects rare GFP-positive cells following DSB induction in the CAPAN-1 cells, indicating that a limited amount of HDR is still possible.

Peptides encoding the third or fourth BRC repeat (BRC3 or BRC4) have recently been shown to disrupt Rad51 nucleoprotein filament formation (Davies et al.,

2001). Additionally, overexpression of BRC4 confers radiation sensitivity to cell lines containing wild-type BRCA2; significantly, a point mutation in the small BRC4 peptide, which has been observed to be a cancer-conferring mutation, abrogates the radiation hypersensitivity (Chen et al., 1999). The decrease in HDR we have observed can be due to improper sequestration of Rad51 by stably expressed products that retain BRC repeats, as for the CAPAN-1 cells (Davies et al., 2001). Significantly, impaired HDR repair is found in the *Brca2*$^{lex1/lex2}$ cells even though Rad51–Brca2 interaction in the nucleus is largely intact. This implies that the truncated Brca2 protein may have a more subtle defect in Rad51 interaction or localization not obvious by coimmunoprecipitation, or that the extreme C terminus plays an additional role in recombination.

Some mutation carriers, such as those with the 6174delT mutation, are expected to express a truncated BRCA2 protein, which like wild-type BRCA2 can interact with Rad51. As yet, it is unknown whether truncated BRCA2, which retains some interaction with Rad51, diminishes HDR in the presence of wild-type BRCA2. A heterozygote phenotype for viability or tumorigenesis has not been reported in mice with targeted *Brca2* alleles, and thus far human tumors derived from *BRCA2* mutation carriers consistently reveal loss of the wild-type allele. However, more subtle changes, such as in breast and ovary morphology, have been described in mice heterozygous for either *Brca1* or *Brca2* mutations, and these changes may be exacerbated by carcinogen exposure (Bennett et al., 2000). As well, it has been reported that cells from *BRCA1* and *BRCA2* mutation carriers are more radiosensitive than cells from wild-type individuals (Foray et al., 1999). Given the sensitivity and technical ease of the DSB repair assay used in this study, the efficiency of HDR in carriers of various *BRCA2* mutations can be explored.

The recombination construct used in this system detects one type of HDR, specifically gene conversion unaccompanied by crossing-over. Noncrossover gene conversion is a common HDR pathway in mammalian cells for the repair of DSBs and employs sister chromatids, homologs, and heterologs, with the primary template for HDR being the sister chromatid (Moynahan and Jasin, 1997; Liang et al., 1998; Richardson et al., 1998; Johnson et al., 1999; Johnson and Jasin, 2000). The DR-GFP substrate, by analogy to other substrates, is believed to provide a measure of both unequal sister chromatid and intrachromatid recombination (Pierce et al., 1999; Johnson and Jasin, 2000), which leads us to propose that BRCA2 has a general role in sister chromatid recombination in proliferating cells. Consistent with a role for BRCA2 following DNA replication, mRNA expression peaks at the G1/S boundary (Rajan et al., 1996; Tashiro et al., 1996; Vaughn et al., 1996), with protein levels increasing as cells enter S phase (Bertwistle et al., 1997; Su et al., 1998). Rad51 shows a similar cell cycle–dependent expression (Yamamoto et al., 1996). Recent studies in *E. coli* have demonstrated that the main function of homologous recombination under normal growth conditions is to restart stalled replication forks (Cox et al., 2000). Direct evidence for a similar role in mammalian cells is not available; however, the lethality of *Rad51*, *Brca1*, and *Brca2* null mutations and the inhibition of cell division upon *Rad51* downregulation (Taki et al., 1996) support such a role for homologous recombination in mammalian cells.

In addition to homologous recombination, DSBs can also be repaired efficiently in mammalian cells by nonhomologous mechanisms (Liang et al., 1998). Both of these repair pathways are implicated in the maintenance of genetic integrity, as cells with homologous or nonhomologous repair defects exhibit gross chromosomal rearrangements (Shen et al., 1998; Cui et al., 1999; Karanjawala et al., 1999; Difilippantonio et al., 2000; Gao et al., 2000), including cells with hypomorphic *Brca2* alleles (Patel et al., 1998; Lee et al., 1999; Yu et al., 2000). That the HDR deficiency is responsible for the genomic instability of Brca2-deficient cells is supported by their apparent proficiency in nonhomologous repair, as determined by V(D)J recombination (Patel et al., 1998) and in vitro end-joining assays (Yu et al., 2000). Although the precise etiology of gross chromosomal rearrangements is not understood, translocations were recently shown to occur between two broken chromosomes in normal cells (Richardson and Jasin, 2000). The translocations arose by nonhomologous end-joining and simple annealing at homologous repeats, but not by gene conversion repair (Richardson and Jasin, 2000). It is possible, therefore, that when HDR is disrupted, DSBs usually repaired by gene conversion are instead repaired by other mechanisms that are more prone to giving rise to translocations and other gross chromosomal rearrangements.

The cellular response to chromosome breaks, including which pathway to repair, may be determined by the cell cycle phase, differentiation status of the cell, and the tissue type (Gao et al., 1998; Takata et al., 1998; Essers et al., 2000). Cells that have exited the cell cycle may be more dependent on nonhomologous repair, whereas cells that are self-renewing, such as during embryogenesis and in some adult tissues, may be more dependent on HDR to repair DSBs that arise during cell division. Whether the tissue specificity seen in hereditary breast cancer predisposition is attributable to a dependence on HDR during key developmental periods or during renewal of cycling epithelial stem cells is an important area for future investigation.

BRCA2, unlike BRCA1, has relatively few alternative hypotheses as to its tumor suppressor function (Welcsh et al., 2000). The striking chromosomal instability phenotype that accompanies HDR deficiencies is a hallmark of human solid tumors, including *BRCA2*-associated tumors (Tirkkonen et al., 1997). The profound defect in HDR of chromosome breaks in *BRCA2* mutant cells confirms a caretaker function for BRCA2 in protecting genomic integrity through efficient repair of DNA damage by homologous recombination.

Experimental Procedures

DNA Manipulations

The p59xDR-GFP6- and p59xDR-GFP4 *pim1*–targeting vectors were constructed by modifying the previously described gene-targeting vector, p59 (te Riele et al., 1990), to contain XhoI sites flanking the targeting arms (p59x) and the DR-GFP recombination substrate (Pierce et al., 1999). The phHPRT-DR-GFP plasmid was digested with AvrII, and the ends were filled in by Klenow polymerase, followed by digestion with SspI. The 6.7 kb fragment containing DR-

GFP was cloned into the p59x-targeting vector at a unique SmaI site 30 bp downstream of the *hyg*-coding sequences. Constructs containing DR-GFP in both the forward and reverse orientations relative to the *hyg* gene were created (p59DR-GFP6 and p59DR-GFP4, respectively). The targeting fragments were obtained by XhoI digestion.

Cell Transfections and Southern Analysis

For stable transfection, CAPAN-1 cells were electroporated at 800 V/3 μF with 75 μg of the SacI/KpnI fragment from phHPRT-DR-GFP, followed by selection after 48 hr in 0.4 μg/ml puromycin. Puromycin-resistant clones were selected and expanded 21 to 30 days later. Southern blots of genomic DNA from these clones were probed with a radiolabeled 1.4 kb HpaI-NarI GFP fragment from pNZE-CAG. CAPAN-1 clones 4, 5, 8, 11, and 23 were confirmed using PstI, HindIII, BglII, and SpeI analysis to have integrated an intact DR-GFP fragment. Overall, 13% of the analyzed puromycin-resistant CAPAN-1 clones had randomly integrated an intact DR-GFP repair substrate. The CAPAN-1 6174delT mutation was verified by DNA sequencing.

For gene targeting, ES cells were electroporated with 75 μg of linear targeting fragment from p59xDR-GFP, followed by selection after 48 hr in 110 μg/ml hygromycin and 1.0 μg/ml puromycin. For DSB repair assays, actively growing cells were electroporated at 250 V/960 μF with 30 to 50 μg of pCBASce (Richardson et al., 1998), mock DNA, or pNZE-CAG (Pierce et al., 1999), and plated in nonselective media. Cells were trypsinized at the indicated times and analyzed by flow cytometry. Data were analyzed with Lysis software.

For physical confirmation of HDR, 1×10^8 ES cells were transfected with 100 μg of pCBASce, and 48 hr afterwards, transfection cells were sorted based on GFP expression. Collections of GFP-negative and GFP-positive cells were expanded. Digested genomic DNA was probed with the 1.4 kb GFP fragment as depicted in Figure 4B.

Protein Manipulations

Cytoplasmic and nuclear fractions were prepared in buffers A and C and the nuclear fraction was dialyzed in buffer D, as described (Lee et al., 1994). Total protein content was determined by Bio-Rad DC protein assay. For Western blot analysis of Brca2 protein, 100 μg of fractionated lysate was electrophoresed by 4.5% SDS-PAGE and probed with an anti-BRCA2 Ab-2 antibody (Oncogene Research). For coimmunoprecipitation, 1 mg of cytoplasmic extract and 500 μg of nuclear extract were immunoprecipitated with 1 mg of an anti-BRCA2 antibody and separated by 10% SDS-PAGE. The probe was an anti-Rad51 antibody (a gift of Steve West).

Acknowledgments

We thank Paul Hasty and Lexicon Genetics for the gift of the *Brca2*$^{lex1/lex2}$ cells. This work was supported by the Department of the Army (DAMD17-98-1-8334) and the National Institutes of Health Specialized Program of Research Excellence in breast cancer (1P50CA68425).

Received August 24, 2000; revised November 30, 2000.

References

Abbott, D.W., Freeman, M.L., and Holt, J.T. (1998). Double-strand break repair deficiency and radiation sensitivity in BRCA2 mutant cancer cells. J. Natl. Cancer Inst. *90*, 978–985.

Abbott, D.W., Thompson, M.E., Robinson-Benion, C., Tomlinson, G., Jensen, R.A., and Holt, J.T. (1999). BRCA1 expression restores radiation resistance in BRCA1-defective cancer cells through enhancement of transcription-coupled DNA repair. J. Biol. Chem. *274*, 18808–18812.

Bennett, L.M., McAllister, K.A., Malphurs, J., Ward, T., Collins, N.K., Seely, J.C., Gowen, L.C., Koller, B.H., Davis, B.J., and Wiseman, R.W. (2000). Mice heterozygous for a Brca1 or Brca2 mutation display distinct mammary gland and ovarian phenotypes in response to diethylstilbestrol. Cancer Res. *60*, 3461–3469.

Bertwistle, D., Swift, S., Marston, N.J., Jackson, L.E., Crossland, S., Crompton, M.R., Marshall, C.J., and Ashworth, A. (1997). Nuclear location and cell cycle regulation of the BRCA2 protein. Cancer Res. *57*, 5485–5488.

Bhattacharyya, A., Ear, U.S., Koller, B.H., Weichselbaum, R.R., and Bishop, D.K. (2000). The breast cancer-susceptibility gene BRCA1 is required for subnuclear assembly of Rad51 and survival following treatment with the DNA crosslinking agent cisplatin. J. Biol. Chem. *275*, 23899–23903.

Bishop, D.K., Ear, U., Bhattacharyya, A., Calderone, C., Beckett, M., Weichselbaum, R.R., and Shinohara, A. (1998). Xrcc3 is required for assembly of Rad51 complexes in vivo. J. Biol. Chem. *273*, 21482–21488.

Chen, J., Silver, D.P., Walpita, D., Cantor, S.B., Gazdar, A.F., Tomlinson, G., Couch, F.J., Weber, B.L., Ashley, T., Livingston, D.M., and Scully, R. (1998a). Stable interaction between the products of the BRCA1 and BRCA2 tumor suppressor genes in mitotic and meiotic cells. Mol. Cell *2*, 317–328.

Chen, P.L., Chen, C.F., Chen, Y., Xiao, J., Sharp, Z.D., and Lee, W.H. (1998b). The BRC repeats in BRCA2 are critical for RAD51 binding and resistance to methyl methanesulfonate treatment. Proc. Natl. Acad. Sci. USA *95*, 5287–5292.

Chen, C.F., Chen, P.L., Zhong, Q., Sharp, Z.D., and Lee, W.H. (1999). Expression of BRC repeats in breast cancer cells disrupts the BRCA2-Rad51 complex and leads to radiation hypersensitivity and loss of G(2)/M checkpoint control. J. Biol. Chem. *274*, 32931–32935.

Connor, F., Bertwistle, D., Mee, P.J., Ross, G.M., Swift, S., Grigorieva, E., Tybulewicz, V.L., and Ashworth, A. (1997). Tumorigenesis and a DNA repair defect in mice with a truncating Brca2 mutation. Nat. Genet. *17*, 423–430.

Cox, M.M. (1999). Recombinational DNA repair in bacteria and the RecA protein. Prog. Nucleic Acid Res. Mol. Biol. *63*, 311–366.

Cox, M.M., Goodman, M.F., Kreuzer, K.N., Sherratt, D.J., Sandler, S.J., and Marians, K.J. (2000). The importance of repairing stalled replication forks. Nature *404*, 37–41.

Cui, X., Brenneman, M., Meyne, J., Oshimura, M., Goodwin, E.H., and Chen, D.J. (1999). The XRCC2 and XRCC3 repair genes are required for chromosome stability in mammalian cells. Mutat. Res. *434*, 75–88.

Davies, A.A., Masson, J.-Y., McIlwraith, M.J., Stasiak, A.Z., Stasiak, A., Venkitaraman, A.R., and West, S.C. BRCA2 controls the RAD51 DNA repair protein. Mol. Cell *7*, this issue, 273–282.

Difilippantonio, M.J., Zhu, J., Chen, H.T., Meffre, E., Nussenzweig, M.C., Max, E.E., Ried, T., and Nussenzweig, A. (2000). DNA repair protein Ku80 suppresses chromosomal aberrations and malignant transformation. Nature *404*, 510–514.

Dronkert, M.L., Beverloo, H.B., Johnson, R.D., Hoeijmakers, J.H., Jasin, M., and Kanaar, R. (2000). Mouse RAD54 affects DNA double-strand break repair and sister chromatid exchange. Mol. Cell. Biol. *20*, 3147–3156.

Essers, J., Hendriks, R.W., Swagemakers, S.M., Troelstra, C., de Wit, J., Bootsma, D., Hoeijmakers, J.H., and Kanaar, R. (1997). Disruption of mouse RAD54 reduces ionizing radiation resistance and homologous recombination. Cell *89*, 195–204.

Essers, J., van Steeg, H., de Wit, J., Swagemakers, S.M., Vermeij, M., Hoeijmakers, J.H., and Kanaar, R. (2000). Homologous and non-homologous recombination differentially affect DNA damage repair in mice. EMBO J. *19*, 1703–1710.

Foray, N., Randrianarison, V., Marot, D., Perricaudet, M., Lenoir, G., and Feunteun, J. (1999). γ-rays-induced death of human cells carrying mutations of BRCA1 or BRCA2. Oncogene *18*, 7334–7342.

Friedman, L.S., Thistlethwaite, F.C., Patel, K.J., Yu, V.P., Lee, H., Venkitaraman, A.R., Abel, K.J., Carlton, M.B., Hunter, S.M., Colledge, W.H., et al. (1998). Thymic lymphomas in mice with a truncating mutation in Brca2. Cancer Res. *58*, 1338–1343.

Gao, Y., Chaudhuri, J., Zhu, C., Davidson, L., Weaver, D.T., and Alt, F.W. (1998). A targeted DNA-PKcs-null mutation reveals DNA-PK-independent functions for KU in V(D)J recombination. Immunity *9*, 367–376.

Gao, Y., Ferguson, D.O., Xie, W., Manis, J.P., Sekiguchi, J., Frank,

K.M., Chaudhuri, J., Horner, J., DePinho, R.A., and Alt, F.W. (2000). Interplay of p53 and DNA-repair protein XRCC4 in tumorigenesis, genomic stability and development. Nature *404*, 897–900.

Goggins, M., Schutte, M., Lu, J., Moskaluk, C.A., Weinstein, C.L., Petersen, G.M., Yeo, C.J., Jackson, C.E., Lynch, H.T., Hruban, R.H., and Kern, S.E. (1996). Germline BRCA2 gene mutations in patients with apparently sporadic pancreatic carcinomas. Cancer Res. *56*, 5360–5364.

Gowen, L.C., Avrutskaya, A.V., Latour, A.M., Koller, B.H., and Leadon, S.A. (1998). BRCA1 required for transcription-coupled repair of oxidative DNA damage. Science *281*, 1009–1012.

Hakem, R., de la Pompa, J.L., Sirard, C., Mo, R., Woo, M., Hakem, A., Wakeham, A., Potter, J., Reitmair, A., Billia, F., et al. (1996). The tumor suppressor gene *Brca1* is required for embryonic cellular proliferation in the mouse. Cell *85*, 1009–1023.

Jeggo, P.A. (1998). DNA breakage and repair. Adv. Genet. *38*, 185–218.

Johnson, R.D., and Jasin, M. (2000). Sister chromatid gene conversion is a prominent double-strand break repair pathway in mammalian cells. EMBO J. *19*, 3398–3407.

Johnson, R.D., Liu, N., and Jasin, M. (1999). Mammalian XRCC2 promotes the repair of DNA double-strand breaks by homologous recombination. Nature *401*, 397–399.

Karanjawala, Z.E., Grawunder, U., Hsieh, C.L., and Lieber, M.R. (1999). The nonhomologous DNA end joining pathway is important for chromosome stability in primary fibroblasts. Curr. Biol. *9*, 1501–1504.

Lee, H., Trainer, A.H., Friedman, L.S., Thistlethwaite, F.C., Evans, M.J., Ponder, B.A., and Venkitaraman, A.R. (1999). Mitotic checkpoint inactivation fosters transformation in cells lacking the breast cancer susceptibility gene, Brca2. Mol. Cell *4*, 1–10.

Lee, K.A.W., Zerivitz, K., and Akusjarvl, G. (1994). Small-scale preparation of nuclear extracts from mammalian cells. In Cell Biology: A Laboratory Handbook, vol. 1, J.E. Celis, ed. (San Diego, CA: Academic Press), pp. 668–670.

Liang, F., Han, M., Romanienko, P.J., and Jasin, M. (1998). Homology-directed repair is a major double-strand break repair pathway in mammalian cells. Proc. Natl. Acad. Sci. USA *95*, 5172–5177.

Lim, D.-S., and Hasty, P. (1996). A mutation in mouse rad51 results in an early embryonic lethal that is suppressed by a mutation in p53. Mol. Cell. Biol. *16*, 7133–7143.

Liu, C.Y., Fleskin-Nikitin, A., Li, S., Zeng, Y., and Lee, W.H. (1996). Inactivation of the mouse BRCA1 gene leads to failure in the morphogenesis of the egg cylinder in early postimplantation development. Genes Dev. *10*, 1835–1843.

Ludwig, T., Chapman, D.L., Papaioannou, V.E., and Efstratiadis, A. (1997). Targeted mutations of breast cancer susceptibility gene homologs in mice: lethal phenotypes of Brca1, Brca2, Brca1/Brca2, Brca1/p53, and Brca2/p53 nullizygous embryos. Genes Dev. *11*, 1226–1241.

Marmorstein, L.Y., Ouchi, T., and Aaronson, S.A. (1998). The BRCA2 gene product functionally interacts with p53 and RAD51. Proc. Natl. Acad. Sci. USA *95*, 13869–13874.

Mizuta, R., LaSalle, J.M., Cheng, H.L., Shinohara, A., Ogawa, H., Copeland, N., Jenkins, N.A., Lalande, M., and Alt, F.W. (1997). RAB22 and RAB163/mouse BRCA2: proteins that specifically interact with the RAD51 protein. Proc. Natl. Acad. Sci. USA *94*, 6927–6932.

Morimatsu, M., Donoho, G., and Hasty, P. (1998). Cells deleted for Brca2 COOH terminus exhibit hypersensitivity to γ-radiation and premature senescence. Cancer Res. *58*, 3441–3447.

Moynahan, M.E., and Jasin, M. (1997). Loss of heterozygosity induced by a chromosomal double-strand break. Proc. Natl. Acad. Sci. USA *94*, 8988–8993.

Moynahan, M.E., Chiu, J.W., Koller, B.H., and Jasin, M. (1999). Brca1 controls homology-directed repair. Mol. Cell *4*, 511–518.

Pâques, F., and Haber, J.E. (1999). Multiple pathways of recombination induced by double-strand breaks in *Saccharomyces cerevisiae*. Microbiol. Mol. Biol. Rev. *63*, 349–404.

Patel, K.J., Vu, V.P., Lee, H., Corcoran, A., Thistlethwaite, F.C., Evans, M.J., Colledge, W.H., Friedman, L.S., Ponder, B.A., and Venkitaraman, A.R. (1998). Involvement of Brca2 in DNA repair. Mol. Cell *1*, 347–357.

Pierce, A.J., Johnson, R.D., Thompson, L.H., and Jasin, M. (1999). XRCC3 promotes homology-directed repair of DNA damage in mammalian cells. Genes Dev. *13*, 2633–2638.

Rahman, N., and Stratton, M.R. (1998). The genetics of breast cancer susceptibility. Annu. Rev. Genet. *32*, 95–121.

Rajan, J.V., Wang, M., Marquis, S.T., and Chodosh, L.A. (1996). Brca2 is coordinately regulated with Brca1 during proliferation and differentiation in mammary epithelial cells. Proc. Natl. Acad. Sci. USA *93*, 13078–13083.

Richardson, C., and Jasin, M. (2000). Frequent chromosomal translocations induced by DNA double-strand breaks. Nature *405*, 697–700.

Richardson, C., Moynahan, M.E., and Jasin, M. (1998). Double-strand break repair by interchromosomal recombination: suppression of chromosomal translocations. Genes Dev. *12*, 3831–3842.

Scully, R., Chen, J., Plug, A., Xiao, Y., Weaver, D., Feunteun, J., Ashley, T., and Livingston, D.M. (1997). Association of BRCA1 with Rad51 in mitotic and meiotic cells. Cell *88*, 265–275.

Sharan, S.K., and Bradley, A. (1997). Murine Brca2: sequence, map position, and expression pattern. Genomics *40*, 234–241.

Sharan, S.K., Morimatsu, M., Albrecht, U., Lim, D.-S., Regel, E., Dinh, C., Sands, A., Eichele, G., Hasty, P., and Bradley, A. (1997). Embryonic lethality and radiation hypersensitivity mediated by Rad51 in mice lacking *Brca2*. Nature *386*, 804–810.

Shen, S.X., Weaver, Z., Xu, X., Li, C., Weinstein, M., Chen, L., Guan, X.Y., Ried, T., and Deng, C.X. (1998). A targeted disruption of the murine Brca1 gene causes γ-irradiation hypersensitivity and genetic instability. Oncogene *17*, 3115–3124.

Spain, B.H., Larson, C.J., Shihabuddin, L.S., Gage, F.H., and Verma, I.M. (1999). Truncated BRCA2 is cytoplasmic: implications for cancer-linked mutations. Proc. Natl. Acad. Sci. USA *96*, 13920–13925.

Su, L.K., Wang, S.C., Qi, Y., Luo, W., Hung, M.C., and Lin, S.H. (1998). Characterization of BRCA2: temperature sensitivity of detection and cell-cycle regulated expression. Oncogene *17*, 2377–2381.

Suzuki, A., de la Pompa, J.L., Hakem, R., Elia, A., Yoshida, R., Mo, R., Nishina, H., Chuang, T., Wakeham, A., Itie, A., et al. (1997). Brca2 is required for embryonic cellular proliferation in the mouse. Genes Dev. *11*, 1242–1252.

Takata, M., Sasaki, M.S., Sonoda, E., Morrison, C., Hashimoto, M., Utsumi, H., Yamaguchi-Iwai, Y., Shinohara, A., and Takeda, S. (1998). Homologous recombination and non-homologous end-joining pathways of DNA double-strand break repair have overlapping roles in the maintenance of chromosomal integrity in vertebrate cells. EMBO J. *17*, 5497–5508.

Taki, T., Ohnishi, T., Yamamoto, A., Hiraga, S., Arita, N., Izumoto, S., Hayakawa, T., and Morita, T. (1996). Antisense inhibition of the RAD51 enhances radiosensitivity. Biochem. Biophys. Res. Commun. *223*, 434–438.

Tan, T.L., Essers, J., Citterio, E., Swagemakers, S.M., de Wit, J., Benson, F.E., Hoeijmakers, J.H., and Kanaar, R. (1999). Mouse Rad54 affects DNA conformation and DNA-damage-induced Rad51 foci formation. Curr. Biol. *9*, 325–328.

Tashiro, S., Kotomura, N., Shinohara, A., Tanaka, K., Ueda, K., and Kamada, N. (1996). S phase specific formation of the human Rad51 protein nuclear foci in lymphocytes. Oncogene *12*, 2165–2170.

te Riele, H., Maandag, E.R., Clarke, A., Hooper, M., and Berns, A. (1990). Consecutive inactivation of both alleles of the *pim-1* proto-oncogene by homologous recombination in embryonic stem cells. Nature *348*, 649–651.

Tirkkonen, M., Johannsson, O., Agnarsson, B.A., Olsson, H., Ingvarsson, S., Karhu, R., Tanner, M., Isola, J., Barkardottir, R.B., Borg, A., and Kallioniemi, O.P. (1997). Distinct somatic genetic changes associated with tumor progression in carriers of BRCA1 and BRCA2 germ-line mutations. Cancer Res. *57*, 1222–1227.

Tsuzuki, T., Fujii, Y., Sakumi, K., Tominaga, Y., Nakao, K., Sekiguchi, M., Matsushiro, A., Yoshimura, Y., and Morita, T. (1996). Targeted

disruption of the Rad51 gene leads to lethality in embryonic mice. Proc. Natl. Acad. Sci. USA *93*, 6236–6340.

Vaughn, J.P., Cirisano, F.D., Huper, G., Berchuck, A., Futreal, P.A., Marks, J.R., and Iglehart, J.D. (1996). Cell cycle control of BRCA2. Cancer Res. *56*, 4590–4594.

Welcsh, P.L., Owens, K.N., and King, M.C. (2000). Insights into the functions of BRCA1 and BRCA2. Trends Genet. *16*, 69–74.

Wong, A.K.C., Pero, R., Ormonde, P.A., Tavtigian, S.V., and Bartel, P.L. (1997). RAD51 interacts with the evolutionarily conserved BRC motifs in the human breast cancer susceptibility gene brca2. J. Biol. Chem. *272*, 31941–31944.

Yamamoto, A., Taki, T., Yagi, H., Habu, T., Yoshida, K., Yoshimura, Y., Yamamoto, K., Matsushiro, A., Nishimune, Y., and Morita, T. (1996). Cell cycle-dependent expression of the mouse Rad51 gene in proliferating cells. Mol. Gen. Genet. *251*, 1–12.

Yano, K., Morotomi, K., Saito, H., Kato, M., Matsuo, F., and Miki, Y. (2000). Nuclear localization signals of the BRCA2 protein. Biochem. Biophys. Res. Commun. *270*, 171–175.

Yu, V.P., Koehler, M., Steinlein, C., Schmid, M., Hanakahi, L.A., van Gool, A.J., West, S.C., and Venkitaraman, A.R. (2000). Gross chromosomal rearrangements and genetic exchange between nonhomologous chromosomes following BRCA2 inactivation. Genes Dev. *14*, 1400–1406.

Yuan, S.S., Lee, S.Y., Chen, G., Song, M., Tomlinson, G.E., and Lee, E.Y. (1999). BRCA2 is required for ionizing radiation-induced assembly of Rad51 complex in vivo. Cancer Res. *59*, 3547–3551.

[CANCER RESEARCH 61, 4842–4850, June 15, 2001]

Homology-directed DNA Repair, Mitomycin-C Resistance, and Chromosome Stability Is Restored with Correction of a *Brca1* Mutation[1]

Mary Ellen Moynahan,[2] Tracy Y. Cui,[3] and Maria Jasin

Department of Medicine [M. E. M.] and Cell Biology Program [T. Y. C., M. J.], Memorial Sloan-Kettering Cancer Center, New York, New York 10021

ABSTRACT

Chromosomal breaks occur spontaneously as a result of normal DNA metabolism and after exposure to DNA-damaging agents. A major pathway involved in chromosomal double-strand break repair is homologous recombination. In this pathway, a DNA sequence with similarity to a damaged chromosome directs the repair of the damage. The protein products of the hereditary breast cancer susceptibility genes, *BRCA1* and *BRCA2*, interact with the Rad51 protein, a central component of homologous repair pathways. We have recently shown that this interaction is significant by demonstrating that *Brca1*- and *BRCA2*-deficient cells are defective in homology-directed chromosomal break repair. We confirm that *Brca1*-deficient embryonic stem (ES) cells are defective in gene targeting and homology-directed repair of an I-*Sce* I-induced chromosome break. The phenotypic paradigm that defines homology-directed repair mutants is extended to these *Brca1*-deficient cells by the demonstration of 100-fold sensitivity to the interstrand cross-linking agent mitomycin-C and spontaneous chromosome instability. Interestingly, although chromosome aberrations were evident, aneuploidy was not observed. Repair phenotypes are partially restored by expression of a *Brca1* transgene, whereas correction of one mutated *Brca1* allele through gene targeting fully restores mitomycin-C resistance and chromosome stability. We conclude that the inability to properly repair strand breaks by homology-directed repair gives rise to defects in chromosome maintenance that promote genetic instability and, it is likely, tumorigenesis.

INTRODUCTION

Individuals who carry mutations in the hereditary breast cancer gene, *BRCA1*, are predisposed to early-onset breast and ovary cancer. Although the relationship to cancer predisposition remains speculative, the BRCA1 protein has been implicated in multiple cellular functions associated with the DNA damage response. These functions include DNA repair (1–3), the cellular response to DNA damage via upstream damage-signaling proteins, and transcriptional regulation of proteins involved in the downstream response to DNA damage. After treatment of cells with DNA damaging agents, BRCA1 is phosphorylated by the signaling proteins ATM, ATR, and Chk2 (4–6) and appears to regulate the expression of genes farther downstream, such as *p21*, *p53*, and *GADD45* (7–9). Biochemical analysis of nuclear extracts demonstrates that the BRCA1 protein is part of a large complex of proteins involved in damage recognition and repair, which has led to the hypothesis that BRCA1 acts as a scaffold to coordinate the cellular response (10).

One type of damage to which mouse and human BRCA1-deficient cells respond abnormally is the DNA DSB.[4] Chromosome DSBs arise from both endogenous processes and exogenous agents such as IR, causing cell death or genomic alterations if not repaired appropriately. *BRCA1* mutant human cells (*i.e.*, HCC1937 cancer cells) are hypersensitive to IR, and this sensitivity is partially relieved (2–3×) by expression of wild-type *BRCA1*. Of note, significant IR sensitivity remains in the BRCA1-complemented HCC1937 cells (3). *Brca1* mutant mouse cell lines, such as the 236.44 ES cell line, are also sensitive to IR, as are *Brca1* mutant embryos (1, 11). In mammalian cells two major repair pathways, homologous recombination and NHEJ, prevent deleterious outcomes after treatment of cells with agents that cause DSBs. The association of Rad51, the eukaryotic homologue of the *Escherichia coli* RecA protein, with BRCA1 in immunoprecipitable complexes, as well as the observed subnuclear localization of BRCA1 with Rad51 in IR-induced foci (12, 13), is highly suggestive of a role for BRCA1 in homology-directed repair (HDR). However, after IR treatment of cells, BRCA1 also colocalizes with the Rad50 complex, which, in yeast, has a role in NHEJ as well as in HDR, raising the possibility of a role for BRCA1 in this DSB repair pathway (14).

We have recently examined DSB repair at the molecular level in the $Brca1^{-/-}$ 236.44 ES cell line to determine the nature of the repair defect. This cell line was constructed through consecutive rounds of gene targeting such that both *Brca1* alleles are mutated by deletion of the 5′ end of exon 11 (15). The targeted alleles are hypomorphs, inasmuch as they express a truncated product arising from an alternatively spliced transcript that skips exon 11 (16). In addition to being hypersensitive to IR, the 236.44 cell line is hypersensitive to cisplatin, has reduced Rad51 focus formation after cisplatin treatment, and is defective in transcription-coupled repair of oxidative damage (1, 17). By examining repair of an endonuclease-generated DSB in this cell line, we demonstrated that HDR is reduced, though NHEJ is not impaired but, rather, slightly elevated (2). Because DSB repair mutants often exhibit spontaneous chromosome instability, there was a concern that additional genomic changes had occurred in the $Brca1^{-/-}$ 236.44 cells, such that the observed repair defects are not fully attributable to loss of wild-type *Brca1*. Partial complementation of these cells by the reintroduction of wild-type *Brca1* has, in fact, not demonstrated a clear restoration of homologous recombination (16).

In the current study, we have examined repair phenotypes of the *Brca1* mutant 236.44 cell line as well as derivative cell lines in which wild-type *Brca1* is reexpressed as a result of either complementation from a *Brca1* transgene or correction of one of the *Brca1* hypomorphic alleles. Using a recombination reporter assay recently developed for the analysis of *Brca2* mutant cells, we show that the 236.44 cell line has impaired HDR of an induced chromosome break and reduced gene targeting, and we confirm that wild-type *Brca1* expression in this cell line restores levels of both types of homologous recombination. We also demonstrate that *Brca1* deficiency results in chromosome instability in ES cells, although not the dramatic instability detected in MEFs. Moreover, *Brca1*-deficient cells exhibit exquisite sensitivity to the interstrand

Received 2//22/01; accepted 5/2/01.

The costs of publication of this article were defrayed in part by the payment of page charges. This article must therefore be hereby marked *advertisement* in accordance with 18 U.S.C. Section 1734 solely to indicate this fact.

[1] This work was supported by DAMD17-98-1-8334 from the Department of the Army, 1P50CA68425 from the NIH Specialized Program of Research Excellence in Breast Cancer, and the Breast Cancer Research Fund.

[2] To whom requests for reprints should be addressed, at Department of Medicine, Memorial Sloan-Kettering Cancer Center, 1275 York Avenue New York, NY 10021. Phone: (212) 639-2168; Fax: (212) 717-3821; E-mail: moynaham@mskcc.org.

[3] Current address: Department of Physiology, University of Michigan, Ann Arbor, MI 48109.

[4] The abbreviations used are: DSB, double-strand break; IR, ionizing radiation; ES, embryonic stem; NHEJ, nonhomologous end-joining; HDR, homology-directed repair; MEF, mouse embryonic fibroblasts; Tg, transgene; pBS, pBluescript; pur^R, puromycin-resistant; hyg^R, hygromycin-resistant; DR-GFP, direct repeat-green fluorescent protein; *neo*, neomycin phosphoribosyl transferase; *hprt*, hypoxanthine phosphoribosyl transferase; XRCC, X-ray cross-complementing repair.

cross-linking agent mitomycin-C, suggesting that this or related DNA-damaging agents may have a highly favorable therapeutic ratio. Notably, restoration of *Brca1* by transgene complementation was less effective at reversing repair defects than correction of a defective *Brca1* allele by gene targeting, presumably because of the difficulty in expressing a physiologically relevant amount of Brca1.

MATERIALS AND METHODS

DNA Manipulations. The p59xDR-GFP6 *pim1*-targeting vector was previously described (18). The targeting fragments were obtained by *Xho*I digestion. The *pBBxAx* transgene and the puromycin-resistant *Brca1*$^{-/-,Tg+}$ cell line containing the *Brca1* cDNA was a gift of Beverly Koller, University of North Carolina, Chapel Hill, NC (16). The plasmid was linearized before transfection. The *pBrca1*$^{+}$*S1Rhyg* (S1R*hyg*) gene-targeting plasmid was constructed by manipulation of a plasmid containing 12.3 kb of murine *Brca1* genomic sequence (gift of Beverly Koller). The plasmid was digested with *Nhe*I-*Spe*I, resulting in a 5.7-kb fragment containing pBS (Promega) and 3′ *Brca1* sequences and a 6.0-kb *Nhe*I-*Spe*I 5′ *Brca1* fragment. These fragments were religated to create *pBrca1Nhe*I*Spe*I, thereby deleting an internal 2.4-kb *Nhe*I *Brca1* fragment. pBS was digested with *Eco*R V-*Hin*cII and religated to delete the *Eco*R V site. *pBrca1Nhe*I-*Spe*I was digested with *Eco*RI to obtain a 7.6-kb *Brca1* fragment, *Not*I linkers were added after Klenow treatment and ligated to *Not*I digested pBS^{delRV} to create *pBrca1*^{Not}. A blunted-ended *hyg-S1neo* fragment (19) was inserted into a unique *Eco*R V site in intron 9 of *pBrca1*^{Not}, creating *pBrca1-RV*^{S1Rhyg}. Orientation of the *hyg* cassette was running in the opposite orientation of *Brca1*. S1R*hyg* was completed by digestion of *pBrca1-RV*^{S1Rhyg} with *Nhe*I and ligation with a 2.4-kb *Nhe*I *Brca1* fragment that had been deleted in an earlier cloning step. Multiple-restriction digests verified the correct orientation of the insert. S1R*hyg* was linearized by digestion with *Not*I before gene targeting.

Cell Transfections and Nucleic Acid Analysis. For stable transfection of pBBxAx, *Brca1*$^{-/-}$ ES cells were cotransfected by electroporation at 800 V/3 μF with 75 μg of the linear fragment from pBBxAx and 25 μg of a phosphoglycerate kinase-puromycin expression plasmid with subsequent selection after 24 h in 1.0 μg/ml puromycin. *pur*^{R} clones were picked and expanded 12–16 days later. Southern blots of genomic DNA from these clones were hybridized with a *Brca1* probe. For gene targeting, ES cells were electroporated with 75 μg of linear targeting fragment from p59xDR-GFP6 with subsequent selection after 48 h in hygromycin 110 μg/ml and puromycin 1.0 μg/ml. *hyg*^{R} and *pur*^{R} clones were picked and expanded 10–12 days later. Southern blots of genomic DNA from these clones were digested with *Hin*cII and hybridized with a radiolabeled *pim1* probe. For *Brca1* correction by gene targeting, *Brca1−/−* ES cells were electroporated with 75 μg of linear *pBrca1*$^{+S1Rhyg}$ targeting fragment with subsequent selection after 24 h in hygromycin 200 μg/ml. *Hyg*^{R} clones were picked and expanded 10–12 days later. Southern blots of genomic DNA from these clones were digested with *Eco*RV and hybridized with a 3′ 1.2-kb *Brca1* probe. For DSB repair assays, actively growing cells were electroporated at 250 V/960 μF with 30–50 μg of pCβASce (20), mock DNA, or pNZE-CAG (21) and plated in nonselective media. Cells were trypsinized at 45–48 h and analyzed by flow cytometry. Data were analyzed with Lysis software. For *Brca1* expression, total mRNA was extracted from actively growing cells by RNAzol (Biotecx Laboratories) treatment. Northern analysis was performed by standard techniques.

Mitomycin-C Clonogenic Survival Assays. For mitomycin-C survival assays, cells were exposed to various mitomycin-C doses for 4 h and then rinsed three times in PBS. The cells were replated and allowed to grow undisturbed for 8–10 days. The colonies were stained and counted. Survival experiments were performed in triplicate.

Metaphase Spreads and Karotype Analysis. For karotype analysis, cells were cultured with 0.05 μg/ml colcemid (Life Technologies, Inc.) for 1.5 h, then trypsinized and resuspended in hypotonic saline (0.075 M KCl) at 37°C for 10 min. The cells were fixed in a 3:1 mix of methanol and acetic acid. Fixed cell suspensions were transferred to glass slides and allowed to air-dry. Metaphase spreads were stained with 4% Giemsa in PBS for 20 min.

RESULTS

Partial Complementation of the Gene-targeting Defect in *Brca1*$^{-/-}$ ES Cells by *Brca1* Transgene Expression. Gene targeting is a measure of the ability of cells to homologously integrate transfected DNA into genetic loci containing sufficient sequence homology to the transfected DNA. Deficiencies in gene targeting, attributable to cellular defects in homologous recombination, have been reported for *Brca1*, *Brca2*, and *Rad54* mutant cell lines, although the precise relationship between homologous integration and HDR is not well understood (2, 18, 22). To investigate both homologous

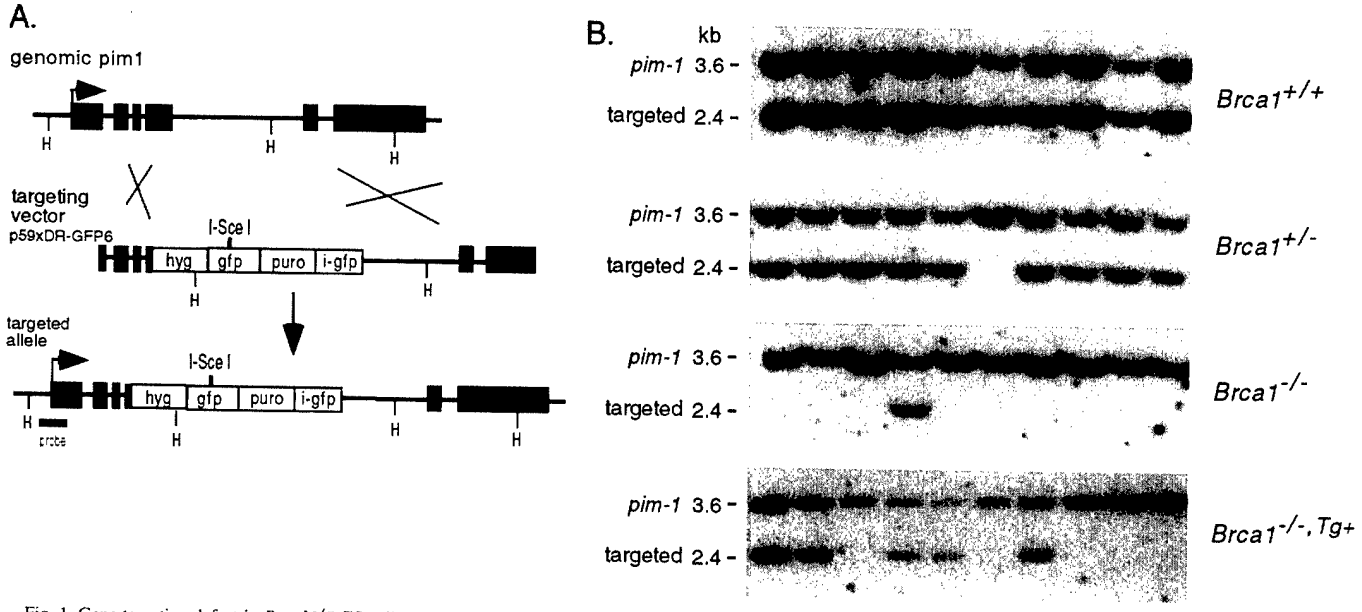

Fig. 1. Gene-targeting defect in *Brca1*$^{-/-}$ ES cells can be partially corrected by *Brca1* transgene expression. *A*, the *pim1* genomic locus undergoes highly efficient gene targeting with the p59xDR-GFP6 vector because of the promoterless integration of hygromycin within *pim1* coding sequences. Clones that are *hyg*^{R} are typically targeted because hygromycin expression from the *pim1* promoter occurs upon homologous integration. Random integration of the p59xDR-GFP6 vector can result in *hyg*^{R} if integration fortuitously occurs adjacent to promoter sequences. Within p59xDR-GFP6 are the *ScGFP* and *iGFP* genes in the same orientation as the *pim1* and *hyg* coding sequences. *H*, *Hin*cII sites. *B*, Southern blot analysis of *hyg*^{R} clones derived from *Brca1*$^{+/+}$, *Brca1*$^{+/-}$, *Brca1*$^{-/-}$, and *Brca1*$^{-/-,Tg+}$ ES cells transfected with the p59xDR-GFP6 targeting vector. DNA from individually expanded clones was digested with *Hin*cII and hybridized with the *pim1* probe (*A*). The wild-type *pim1* allele generates a 3.6-kb *Hin*cII fragment, and the targeted *pim1* allele generates a 2.4 kb fragment.

Table 1 *Gene-targeting efficiency at the pim1 locus*

Cells were electroporated with linearized p59×DR-GFP6 and selected in hygromycin (110 μg/ml) and puromycin (1 μg/ml).

Genotype	Gene-targeting efficiency (no. targeted clones/total analyzed)	FD[a]
Brca1$^{+/+}$	96.7% (58/60)	
Brca1$^{+/-}$	94.1% (48/51)	1.0
Brca1$^{-/-}$	5.9% (2/34)	16.4
Brca1$^{-/-,Tg+}$	61.9% (52/84)	1.6

[a] FD, fold decrease.

recombination pathways, *i.e.,* gene targeting and HDR of a targeted chromosomal break, the DR-GFP reporter substrate was subcloned into the *pim1* gene-targeting vector, p59x, creating p59xDR-GFP6 (Fig. 1*A*; Ref. 18). Gene targeting with the p59x vector is highly efficient, because the selectable hygromycin resistance gene (*hyg*^{R}) is fused in-frame to *pim1* coding sequences such that expression of *hyg*^{R} is dependent on either targeting to the *pim1* locus on chromosome 17 or a fortuitous nonhomologous integration adjacent to promoter sequences of another locus (23). The p59xDR-GFP6 vector additionally contains an intact puromycin resistance gene (*pur*^{R}), which can also be used to select for vector integration events.

In our initial report examining homologous recombination in the *Brca1*$^{-/-}$ 236.44 cell line, we determined that gene targeting was reduced 13- and 23-fold relative to the control *Brca1*$^{+/-}$ cell line, as measured at two distinct genomic loci, *Rb* and *pim1,* respectively (2). To confirm that the defect in gene targeting was attributable to the loss of wild-type Brca1, we electroporated the linearized p59xDR-GFP6 targeting fragment into a *Brca1*$^{-/-,Tg+}$ cell line that is derived from the *Brca1*$^{-/-}$ line, but which expresses full-length mouse *Brca1* from a randomly integrated cDNA at ~10–20% normal *Brca1* levels (Ref. 16 and data not shown). Doubly resistant *hyg*^{R}/*pur*^{R} colonies were selected, and genomic DNA from individual colonies was analyzed by Southern blotting using a *pim1* probe located outside the targeting fragment (Fig. 1*A*). Efficient gene targeting was observed in the *Brca1*$^{+/-}$ cells, with 94% of *hyg*^{R}/*pur*^{R} clones correctly targeted (Fig. 1*B*; Table 1). However, homologous integrations were rarely detected in the *Brca1*$^{-/-}$ cells, with only 6% of the *hyg*^{R}/*pur*^{R} clones correctly targeted, which is a 16-fold lower frequency of gene targeting as compared with *Brca1*$^{+/-}$ cells. This diminished ability to gene target is comparable with the 23-fold lower frequency we originally reported at the *pim1* locus in the *Brca1*$^{-/-}$ cells. The small improvement in gene targeting may be related to the more stringent combined hygromycin and puromycin selection used in the targeting of the p59xDR-GFP6 fragment, because we observed that background colonies observed during hygromycin selection of *Brca*$^{-/-}$ cells were significantly reduced with the combined selection. The addition of puromycin to the hygromycin selective media for *Brca1*$^{+/+}$ and *Brca1*$^{+/-}$ cells did not alter or improve upon the gene targeting frequencies obtained with hygromycin alone (data not shown). The addition of puromycin to the *Brca1*$^{-/-,Tg+}$ would not effect gene targeting, because these cells were selected for *pur*^{R} during the integration of the *Brca1* transgene (16).

In the *Brca1*$^{-/-,Tg+}$ cells, gene targeting was partially restored, whereby homologous integrants were obtained at a frequency of nearly 62% (Fig. 1*B* and Table 1). This is a 10-fold improvement in gene targeting as compared with the *Brca1*$^{-/-}$ mutant cells. However, when compared with the *Brca1*$^{+/-}$ cells, a 1.6-fold decreased targeting efficiency remained in the transgene corrected cell line, suggesting only partial complementation of the gene targeting defect by expression from the *Brca1* transgene.

In this experiment we also examined gene targeting in parental *Brca1*$^{+/+}$ cells, because loss of a single *BRCA1* allele in human cell lines has been implicated in sensitivity to DNA-damaging agents (24). Similar to the *Brca1*$^{+/-}$ cells, 97% of *hyg*^{R}/*pur*^{R} clones were correctly targeted. Thus, mouse cells heterozygous for a *Brca1* mutation have no detectable defect in gene targeting as compared with *Brca1*$^{+/+}$ ES cells. In addition, these results imply that the *Brca1* exon 10–12 splice variant that is expressed in the *Brca1*$^{+/-}$ cells has no detectable dominant-negative effect on gene targeting.

HDR of a Chromosomal DSB in *Brca1*$^{-/-}$ ES Cells Is Also Partially Restored by *Brca1* Transgene Expression. The DR-GFP reporter substrate (21), which was incorporated at the *pim1* locus of cell lines during targeting of the p59xDR-GFP6 vector, measures HDR of an endonuclease-induced DSB by a gene conversion mechanism. It is composed of two differentially mutated *GFP* genes

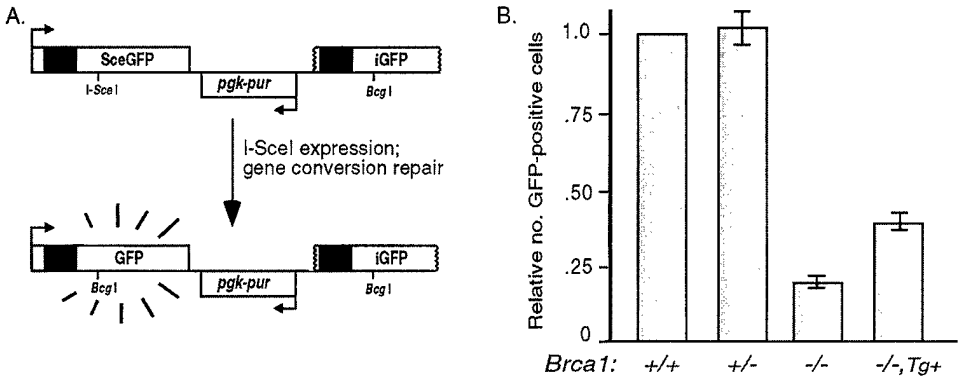

Fig. 2. *Brca1* transgene expression can partially restore HDR of a chromosomal DSB in *Brca1*$^{-/-}$ ES cells. *A,* the recombination repair substrate DR-GFP is composed of two differentially mutated *GFP* genes, *SceGFP* and *iGFP.* When the I-*Sce* I endonuclease is expressed in cells which have targeted the DR-GFP substrate to the *pim1* locus, a DSB will be introduced at the I-*Sce* I site in the *SceGFP* gene. Repair of the DSB by a non-crossover gene conversion with the downstream *iGFP* gene results in reconstitution of a functional *GFP* gene. Because the I-*Sce* I site mutation in the *SceGFP* gene entails 11 bp changes including the introduction of two stop codons, homologous recombination between *SceGFP* and *iGFP* is required to restore a functional *GFP* gene (21). *B,* gene conversion within the DR-GFP substrate as deduced from the percentage of GFP-positive cells. Targeted *Brca1*$^{+/+}$, *Brca1*$^{+/-}$, *Brca1*$^{-/-}$, and *Brca1*$^{-/-,Tg+}$ ES cell lines were transiently transfected with the I-*Sce* I expression vector, pCβASce, negative control DNA, and positive control DNA. The rare occurrence of GFP-positive cells after transfection with negative control DNA (0.00–0.01%) is not shown. ▨, the percentage of GFP-positive cells subsequent to transfection of the I-*Sce* I expression vector normalized to the wild-type *Brca1*$^{+/+}$ cells. I-*Sce* I expression strongly induces the number of GFP-positive *Brca1*$^{+/+}$ and *Brca1*$^{+/-}$ cells, indicating robust DSB repair by gene conversion; however, *Brca1*$^{-/-}$ cells have 6-fold fewer GFP-positive cells, indicating impaired HDR of a DSB by gene conversion ($P < 0.0001$). *Brca1* transgene expression in the *Brca1*$^{-/-,Tg+}$ cells exhibited a 2-fold improvement in HDR of an induced DSB as compared with the *Brca1*$^{-/-}$ cells ($P = 0.032$). This graphical depiction includes quadruplicate experiments wherein three independent clones from each different genotype were analyzed. The number of GFP-positive cells for the three independent clones from each genotype was averaged for each experiment. The percentage of GFP-positive wild-type cells was normalized to one, and the relative frequencies of the other *Brca1* genotypes were calculated; +/+, *Brca1*$^{+/+}$ cells; +/−, *Brca1*$^{+/-}$cells; −/−, *Brca1*$^{-/-}$ cells; and −/−, *Tg*+, *Brca1*$^{-/-,Tg+}$ cells targeted with the p59xDR-GFP6 vector. *Bars,* SE.

oriented as direct repeats and separated by the *pur*^{R} gene (Fig. 2*A*). The *SceGFP* gene is a *GFP* gene that is mutated by 11 bp substitutions to contain the 18 bp recognition sequence for the I-*Sce* I endonuclease. Downstream of *SceGFP* is the 0.8-kb *GFP* fragment *iGFP*, which is a wild-type *GFP* gene truncated at both its 5′ and 3′ ends. Expression of I-*Sce* I in cells that have the DR-GFP substrate integrated into their genome results in a DSB in the chromosome at the position of the I-*Sce* I site. Repair of the induced DSB in *SceGFP* by a non-crossover gene conversion with *iGFP* reconstructs a *GFP*$^+$ gene, expression of which can be scored by cellular fluorescence. Although other DSB repair events at the I-*Sce* I site are possible, they are not detected, because the 11-bp substitutions in the *SceGFP* gene cannot be restored to the wild-type *GFP* sequence except through a templated gene conversion event. Molecular analysis of the DR-GFP substrate in sorted GFP-positive cells after I-*Sce* I expression has verified that cellular green fluorescence, as measured by flow cytometry, results from repair by gene conversion (18, 21).

To analyze HDR in cell lines with various *Brca1* genotypes, several of the p59xDR-GFP6 targeted clones for each genotype were electroporated with the I-*Sce* I expression vector pCβASce to transiently express the I-*Sce* I endonuclease. Electroporated cells were typically examined 48 h later by flow cytometry. GFP-positive cells were undetected or rarely detected (<0.01%) in any of the cell lines in the absence of I-*Sce* I expression (data not shown), indicating that spontaneous intrachromosomal gene conversion is rare. After transfection with pCβASce, however, GFP-positive cells were readily detected in the *Brca1*$^{+/+}$ and *Brca1*$^{+/-}$ cells, indicating robust HDR of the induced DSB. The absolute frequency of GFP positive cells varied between experiments, with a range of 1–4% positive cells, although there was no detectable difference between the *Brca1*$^{+/+}$ and *Brca1*$^{+/-}$ cells when normalized to each other within a particular experiment (Fig. 2*B*). As with gene targeting, therefore, HDR of an induced chromosomal break is not diminished in ES cells containing only one wild-type *Brca1* allele. Proficient HDR in the *Brca1*$^{+/-}$ cells also indicates that the exon 10–12 splice variant arising from the mutated *Brca1* allele does not exhibit a dominant-negative effect on the wild-type *Brca1* allele.

The *Brca1*$^{-/-}$ cells exhibited many fewer GFP-positive cells after I-*Sce* I expression, such that there was a 6-fold decrease in HDR relative to the *Brca1*$^{+/+}$ and *Brca1*$^{+/-}$ cell lines (Fig. 2*B*). This decrease in gene conversion measured by GFP expression is comparable with the previously reported 5–6-fold decrease in gene conversion measured by a PCR-based assay with a *neo* substrate (2). The transgene-complemented *Brca1*$^{-/-,Tg+}$ cells, however, showed a 2-fold increase in HDR over the *Brca1*$^{-/-}$ cells. Thus, HDR was increased by wild-type *Brca1* expression, although, as with gene targeting, it was not completely restored.

Electroporations were also performed with a GFP expression vector to verify that the different cell lines had a similar transfection efficiency. The GFP expression vector that was electroporated, pCAG-NZE, uses the same control elements to express GFP as the pCβASce vector uses to express I-*Sce* I. Electroporated cells were examined by flow cytometry. No difference in GFP expression, which ranged from 44–58%, was detected between any of the *Brca1*$^{+/+}$, *Brca1*$^{+/-}$, *Brca1*$^{-/-}$, and *Brca1*$^{-/-,Tg+}$ targeted cell clones (data not shown), indicating that the transfection efficiency was not appreciably different for these lines.

Brca1-deficient Cells Are Hypersensitive to the DNA Interstrand Cross-linking Agent Mitomycin-C. The first recognized mammalian HDR mutants, the irs1 and irs1SF hamster cell lines deficient for the Rad51-related proteins XRCC2 and XRCC3, respectively, show moderate sensitivity to IR, as do *Brca1*-deficient cells, but an extreme sensitivity to mitomycin-C (25). Mitomycin-C produces several types of DNA damage, one of which is an interstrand DNA cross-link. This lesion could potentiate DSBs through replication fork blockage, producing an intermediate that is much more dependent for repair on HDR than on NHEJ, although the exact mode of repair is unknown (26). To investigate whether *Brca1* deficiency also results in mitomycin-C sensitivity, clonogenic survival assays were performed in the *Brca1*$^{+/+}$, *Brca1*$^{+/-}$, *Brca1*$^{-/-}$, and *Brca1*$^{-/-,Tg+}$ cell lines after exposure to increasing doses of mitomycin-C.

Hypersensitivity was seen at all mitomycin-C doses in the *Brca1*$^{-/-}$ cells as compared with the wild-type and heterozygous *Brca1* cell lines (Fig. 3). The extent of sensitivity to mitomycin-C was dose dependent. At a mitomycin-C concentration of 0.5 μM, which was approximately the LD_{50} for wild-type cells, the *Brca1*$^{-/-}$ cells exhibited a >100-fold increased sensitivity (Fig. 3). No difference in sensitivity to mitomycin-C in the *Brca1*$^{+/-}$ and *Brca1*$^{+/+}$ cell lines was observed at this or other doses. Consistent with the homologous recombination assays, the *Brca1*$^{-/-,Tg+}$ cell lines revealed an intermediate sensitivity to mitomycin-C.

In an attempt to restore wild-type levels of mitomycin-C resistance to the *Brca1*$^{-/-}$ cells, we constructed additional transgene-complemented clones. *Brca1*$^{-/-}$ cells were electroporated with the selectable *pur*^{R} gene and the pBBrpAX expression vector, which expresses mouse *Brca1* from 4 kb of *Brca1* upstream sequences and has a bovine growth hormone polyadenylation signal. This is the same vector previously used to construct the *Brca1*$^{-/-,Tg+}$ cell line (16). *Pur*^{R} clones were analyzed by Northern blotting for *Brca1* expression, and, although some clones did not express *Brca1*, others had levels comparable with the *Brca1*$^{-/-,Tg+}$ cell line (data not shown). Two of these *Brca1*-expressing clones were tested in a mitomycin-C clonogenic survival assay along with a *pur*^{R} clone that did not express *Brca1*. Whereas the nonexpressing clone demonstrated the same hypersensitivity to mitomycin-C as did the parental *Brca1*$^{-/-}$ cell line, the *Brca1*-expressing clones demonstrated a similar intermediate level of mitomycin-C sensitivity that was seen for the *Brca1*$^{-/-,Tg+}$ cell line (data not shown). Thus, we were unable to fully restore wild-type levels of mitomycin-C resistance by transgene complementation.

Correction of the *Brca1* Exon 11 Deletion through Gene Targeting. The incomplete restoration of homologous recombination and mitomycin-C resistance in the *Brca1* transgene-complemented cell

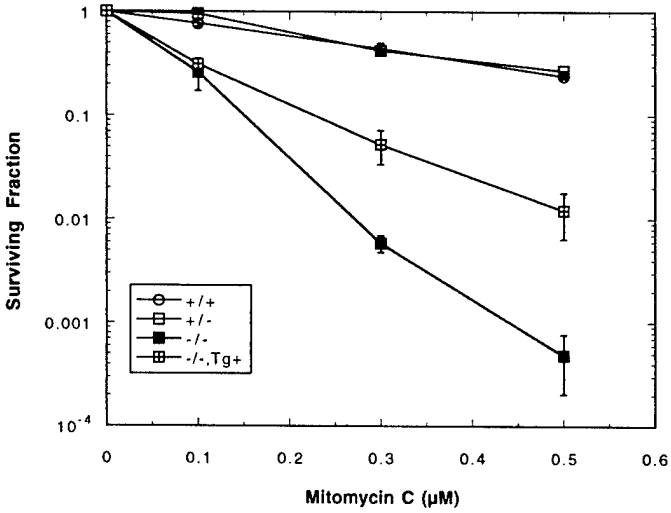

Fig. 3. Brca1$^{-/-}$ cells are hypersensitive to mitomycin-C. Clonogenic survival was assessed after treatment with varying concentrations of mitomycin-C. Four plates from each *Brca1* genotype, as indicated, were assessed for colony formation 8–10 days after exposure to mitomycin-C. The experiments were repeated. *Bars*, SE.

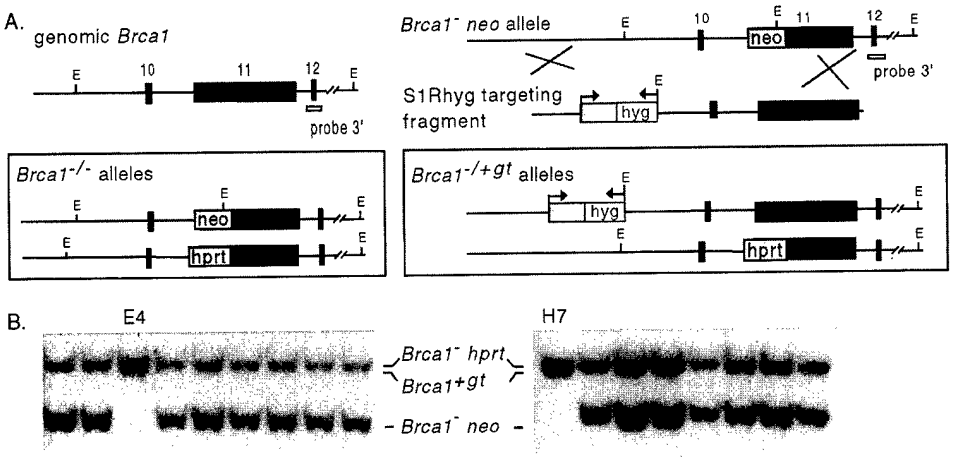

Fig. 4. Correction of the *Brca1*$^{-/-}$ cells through gene targeting. *A*, a portion of genomic *Brca1* at exons 10–12. The genomic structure of the gene-targeted alleles in the *Brca1*$^{-/-}$ cells shows the disruption of exon 11 by *hprt* on one allele and *neo* on the other allele. The targeting fragment, S1Rhyg, has an intact exon 11 with a *hyg* gene inserted at an *Eco*R V site within intron 9 of *Brca1* genomic sequences. Gene targeting of the S1R*hyg* fragment to the *Brca1* locus in the *Brca1*$^{-/-}$ cells can restore wild-type *Brca1* to one allele to create a *Brca1*$^{+gt}$ allele. *B*, Southern blot analysis of *hyg*^{R} clones after transfection with the S1Rhyg fragment. Genomic DNA from 159 *hyg*^{R} clones was digested with *Eco*R V and hybridized to a radio-labeled 3′ *Brca1* probe as indicated in *A*. Two *Brca1*$^{-/+gt}$ clones, E4 and H7, were identified which contained the 11.3-kb S1Rhyg *Brca1* fragment, indicative of correction of the *Brca1*$^{-}$ *neo* allele with the *Brca1*$^{+gt}$ allele. The large fragment-size of the *Brca1*$^{-}$*hprt* and *Brca1*$^{+gt}$ alleles make the separation by size difficult and, therefore, is commonly observed as a doublet by Southern analysis.

lines could be attributable to inadequate expression of *Brca1* or undetected alterations in the *Brca1* transgene upon integration. It is also formally possible that genomic changes occurred in the *Brca1*$^{-/-}$ cell line that contributed to the observed repair defects. This was a particular concern, given the dramatic chromosomal instability observed in MEFs harboring a similar *Brca1* mutation.

To better address the dependence of the repair defects on *Brca1*-deficiency, a gene-targeting fragment was constructed to correct the exon 11 deletion mutation in the *Brca1*$^{-/-}$ 236.44 cell line (Fig. 4*A*). The *Brca1* alleles in this line are disrupted by replacement of the 3′ end of intron 10 and 1.5 kb from the 5′ end of exon 11 with *neo* and *hprt* selectable marker genes. To correct one of these alleles, a targeting fragment was constructed in which the *hyg*^{R} gene was inserted into intron 9 of wild-type murine *Brca1* genomic sequences. Gene targeting of this fragment, termed S1Rhyg, at either *Brca1* allele would therefore restore an intact exon 11, giving rise to a *Brca1*$^{+gt}$ allele. In wild-type ES cells, we found that the S1Rhyg fragment yielded a high targeting efficiency, such that 75–90% of the *hyg*^{R} clones had homologously integrated this fragment at the *Brca1* locus (data not shown). Thus, although gene targeting is substantially reduced in the *Brca1*$^{-/-}$ cell line, the high targeting efficiency of this fragment suggested that we would be able obtain homologous integrations with sufficient screening of *hyg*^{R} clones.

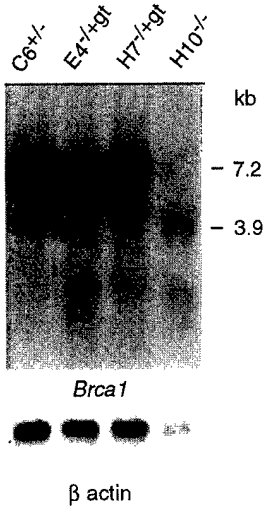

Fig. 5. Expression of *Brca1* is restored in *Brca1*$^{-/+gt}$ cells. Northern blot analysis was performed with 10 μg of total RNA obtained from *Brca1*$^{+/-}$, *Brca1*$^{-/+gt}$, and *Brca1*$^{-/-}$ cells. Endogenous *Brca1* expression results in a 7.2kb mRNA, which is observed in the *Brca1* heterozygote C6 clone and the two *Brca1*$^{-/+gt}$ corrected E4 and H7 clones. The *Brca1*$^{-/-}$ H10 clone is a *hyg*^{R} clone that was obtained from the S1R*hyg* gene-targeting experiment in which the fragment had integrated randomly into the genome and therefore did not correct the *Brca1* mutation. This cell line does not express the 7.2-kb *Brca1* mRNA, but it does express the 3.9-kb *Brca1* exon 10–12 splice variant. Quantitation of mRNA by Phospho-image analysis indicated that the gene-corrected and heterozygote cells expressed wild-type *Brca1* at similar levels. The slightly slower mobility for the H7 *Brca1* mRNA was not seen consistently. A *Brca1* probe containing the sequence from exons 9–11 was used for detection. The blot was rehybridized with a β-actin probe to confirm equal RNA loading.

As the *Brca1*$^{-/-}$ cell lines with the integrated DR-GFP substrate were already *hyg*^{R}, the parental *Brca1*$^{-/-}$ 236.44 cell line was electroporated with the S1Rhyg targeting fragment. *Hyg*^{R} clones were analyzed by Southern blotting using a *Brca1* probe located 3′ to the targeting fragment (Fig. 4*A*). Two of 159 *hyg*^{R} clones yielded *Eco*RV fragments indicative of correction of the *neo* allele (Fig. 4*B*). Whereas most of the clones gave two distinct fragments for the *hprt* and *neo* alleles (12.3 and 5.9 kb, respectively), as in the parental *Brca1*$^{-/-}$ cell line, in the two targeted clones, E4 and H7, the *neo* fragment was replaced with a fragment expected for a targeted *Brca1*$^{+gt}$ *hyg* allele (11.3 kb). Because of the similarity in size of the *hprt* and *hyg* alleles, the blots were reprobed with an *hprt* fragment to determine whether the *hprt* allele was gene-targeted. In each of the clones, the *hprt* allele was still present, indicating that none of the other 157 clones was targeted (data not shown).

Because insertions into the intron of a gene can sometimes disrupt its expression, we determined whether *Brca1* mRNA was restored in the targeted clones by performing Northern blot analysis. *Brca1*$^{+/-}$ cells were found to express the wild-type 7.2-kb *Brca1* mRNA (Fig. 5), which was not present in the *Brca1*$^{-/-}$ cells (data not shown). Rather, a 3.9-kb transcript was seen in the mutant cells that resulted from the exon 10–12 splice. In the E4 and H7 *Brca1*$^{-/+gt}$ clones, the 7.2-kb mRNA was observed, indicating restoration of *Brca1* expression (Fig. 5). Quantitation of *Brca1* expression in these clones indicated that mRNA levels were similar to the *Brca1*$^{+/-}$ cells. A third *hyg*^{R} clone, H10, that was derived from the S1Rhyg targeting experiment but which had randomly integrated the fragment, was also examined for *Brca1* expression. As expected, only the 3.9-kb exon

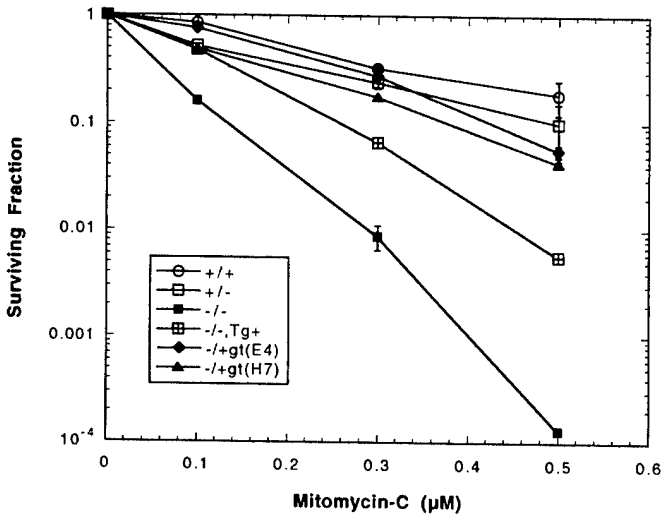

Fig. 6. Mitomycin-C resistance is restored with correction of the *Brca1* mutation. In addition to the $Brca1^{+/+}$, $Brca1^{+/-}$, $Brca1^{-/-}$, and $Brca1^{-/-.\ Tg+}$ cell lines, the two corrected $Brca1^{-/+gt}$ cell were treated with mitomycin-C at various doses. Clonogenic survival assays were performed as described in the legend to Fig. 3. Mitomycin-C resistance is restored to near wild-type levels in the gene-corrected E4 and H7 $Brca1^{-/+gt}$ cell lines. Depicted are the various *Brca1* genotypes.

10–12 variant mRNA was observed in the H10 clone, similar to the parental $Brca1^{-/-}$ cells (Fig. 5).

To determine whether restoration of *Brca1* expression in the $Brca1^{-/+gt}$ cells led to normal levels of mitomycin-C resistance, the E4 and H7 clones were analyzed in clonogenic survival assays together with the control cells. Unlike the transgene complemented lines, restoration was nearly complete in both of the $Brca1^{-/+gt}$ clones, as compared with both wild-type and heterozygote *Brca1* cells (Fig. 6). This functional restoration suggests that the repair defects observed in the $Brca1^{-/-}$ 236.44 cell line are attributable specifically to the *Brca1* mutation rather than to other genetic alterations.

Spontaneous Chromosome Instability in $Brca1^{-/-}$ ES Cells. Chromosome instability in the absence of exogenous DNA-damaging agents seems to be a hallmark of cells with HDR defects. Consistent with this, MEFs and tumors derived from mice that harbor a *Brca1* exon 11 deletion created by lox-cre recombination have marked chromosome instability, including extensive aneuploidy, chromosome breaks, and translocations (11, 27, 28). Because ES cells in some instances manifest different DNA damage responses than fibroblasts, we examined metaphase spreads of ES cell lines carrying different *Brca1* genotypes to determine whether these cells have chromosomal abnormalities. Unlike *Brca1*-deficient MEFs, $Brca1^{-/-}$ ES cells did not exhibit pronounced aneuploidy (data not shown). The average chromosome number in the $Brca1^{-/-}$ cells was 40, which was not significantly different from the wild-type and $Brca1^{+/-}$ cell lines. However, chromosome instability was evident in the *Brca1*-deficient cells, as characterized by an increase in the number of chromosome aberrations (Table 2). The control cell lines expressing wild-type *Brca1*, *i.e.*, $Brca1^{+/+}$, $Brca1^{+/-}$, and corrected $Brca1^{-/+gt}$ cell lines, each had a similar low frequency of observed chromosome aberrations, ~3–4% of metaphases. By contrast, the *Brca1* mutant cells had a substantially increased number, with ~20% of metaphases containing aberrations. Spontaneous chromosomal instability is significantly higher ($P = 0.0079$) in $Brca1^{-/-}$ cells as compared with $Brca1^{+/+}$, $Brca1^{+/-}$ and $Brca1^{-/+gt}$ cells. The increase was attributable to a number of different chromosomal abnormalities, including chromatid breaks and exchanges and chromosome breaks, deletions, and translocations. As seen with other assays, the $Brca1^{-/-Tg+}$ cell lines fell between mutant and wild-type cells. They had ~2-fold fewer aberrations than $Brca1^{-/-}$ cells ($P = 0.043$), but 2–3-fold more aberrations than wild-type cells, in accordance with partial correction of the *Brca1* defect in these cells. This contrasted with the gene-targeted E4 and H7 clones that were fully corrected.

It is plausible that chromosome aneuploidy and multiple aberrations within a cell are better tolerated in a differentiated cell type and extended further when cell checkpoints are eliminated. However, when cells responsible for self-renewal incur chromosome insults, such as the ES cell, it is possible that cell death pathways predominate to limit the propagation of this instability. Although increased cell death was not formally evaluated in this study, a striking small-colony morphology was typically exhibited in the $Brca1^{-/-}$ cell lines as compared with the cell lines that contained a wild-type *Brca1* allele (data not shown). This small-colony morphology was eliminated by correction in the $Brca1^{-/+gt}$ cell lines (data not shown). Cell cycle distribution was evaluated previously (2, 17) and was found to be similar between the $Brca1^{-/-}$and $Brca1^{+/-}$ cell lines and therefore was not likely to be a factor in the etiology of small colonies.

DISCUSSION

These results provide direct evidence that cells containing a *Brca1* mutation have impaired homologous recombination, as measured by

Table 2 *Spontaneous gross chromosomal aberrations in mouse ES cells lines with different Brca1 genotypes*

Brca1 genotype and cell lines	Metaphases analyzed	Metaphases with aberrations (%)	Aberrations/ metaphase	Chromatid		Chromosome				
				Break	Exchange	Break	Int del[a]	ter del	f	trans
+/+										
ES-A12	100	3.0	0.03	1	0	0	0	0	1	1
ES-B12	100	3.0	0.04	0	0	1	0	0	1	2
+/−										
310.7-C6	100	3.0	0.03	0	1	0	0	0	0	2
310.7-H2	100	4.0	0.04	0	1	0	0	1	0	2
−/−										
236.44-A4	100	20.0	0.26	7	8	2	3	0	1	5
236.44-F6	100	20.0	0.21	0	4	1	3	2/85[b]	1	10
−/−,Tg+										
KC-B5	100	8.0	0.08	0	3	0	1	1/38[b]	0	3
KC-E4	100	11.0	0.14	1	1	1	0	6	3	2
−/+gt										
E4	100	4.0	0.04	0	0	0	0	0	0	4
H7	100	3.0	0.03	1	0	0	0	0	0	2
−/−[c]										
H10	100	21.0	0.23	2	2	2	0	12	1	4

[a] Int del, interstitial deletion; ter del, terminal deletion; f, fragment; trans, translocation.
[b] Repetitive aberration (number of repetitive aberrations/number of metaphases with repetitive aberrations.
[c] Random integrant derived from gene correction experiment.

gene targeting and, importantly, HDR of a chromosome break. Moreover, *Brca1* deficiency results in mitomycin-C sensitivity, which is more profound than the previously published IR and cisplatin sensitivities (1, 17). A substantial increase in gross chromosomal aberrations was also observed, although aneuploidy was not evident. These latter defects of cross-linking agent sensitivity and genomic instability are fully attributable to *Brca1* deficiency, and it is probable that the HDR defect in this cell line is also completely attributable to *Brca1* deficiency.

Mammalian cell lines identified to have substantially impaired HDR defects, *i.e.,* the *XRCC2* and *XRCC3* mutants, were originally characterized on the basis of their weak IR sensitivity but substantial mitomycin-C sensitivity and a high frequency of both spontaneous and induced chromosomal aberrations (25, 29). The repair phenotypes arising from *Brca1* mutation described in this report are similar to those found in classical HDR mutants, and recent results suggest that similar phenotypes arise from *Brca2* mutation (30). These phenotypes may define the paradigm for HDR mutants and provide a contrast to NHEJ mutants, for which severe IR sensitivity and little or no cross-linking agent sensitivity is observed (26, 31). Induced chromosomal aberrations are also frequent in NHEJ mutants, although spontaneous instability is not uniformly observed in cells with reduced NHEJ (32–35). An additional emerging characteristic that may be attributable to defects in HDR is that of centrosome abnormalities, which have been observed in *XRCC2, XRCC3, BRCA1,* and *BRCA2* mutant cells, in contrast with the lack of abnormalities in cells defective for NHEJ (27, 34, 36, 37). Thus, a proportion of gross chromosome abnormalities may result from chromosome missegregation. Although aneuploidy was not evident in *Brca1*-deficient ES cells, it is commonly observed in other HDR mutant cells.

Gross chromosomal instability is observed in MEFs and tumor cells derived from mice harboring *Brca1* hypomorphic alleles (11, 27, 28). However, as shown here, ES cells harboring similar hypomorphic *Brca1* alleles have chromosome instability that is much less pronounced, suggesting that MEFs (as well as tumors) may be inherently prone to accumulate damage. The ES cell ultimately is required to generate all tissues of the adult organism and therefore may be exquisitely sensitive to a very low threshold of genetic change. As the cell cycle distribution of the mutant ES cells is normal, increased cell death may eliminate cells with unrepaired damage. Recently it has been shown that although p53 accumulates during stalled DNA replication, it is functionally impaired, suggesting repression of the p53 response during S-phase arrest (38). One possibility for the lack of aneuploidy is that p53 function is less tightly regulated during replication blocks in ES cells, resulting in the elimination of cells when unrepaired chromosome breaks are encountered.

We found that correction of a mutant *Brca1* allele led to complete rescue of the repair phenotypes, yet transgene expression of *Brca1*, even from a *Brca1* promoter, led to only partial complementation. It remains uncertain why transgene rescue was incomplete; however, these results point to the difficulty of ectopic expression and suggest that a larger genomic region is necessary for proper regulation of *Brca1* gene expression. Previously, transgene expression was shown to be insufficient for even partial restoration of normal gene-targeting efficiency in the *Brca1* mutant cell line (16). It is possible that targeting at loci tested in this previous study had a more stringent requirement for normal *Brca1* levels than the *pim1* locus. Nevertheless, *Brca1* transgene expression led to a robust 10-fold improvement in *pim1* targeting, which was confirmed by molecular analysis.

We expect that HDR of a chromosomal DSB is more physiologically relevant than gene targeting. In HDR assays, *Brca1* transgene expression led to increased recombination, improving it to an intermediate level as seen for the other repair phenotypes. DSBs arising from exogenous sources like I-*Sce* I are potent inducers of recombination between sister-chromatids, which are templates for repair after DNA replication (39). DSBs may also arise during normal S-phase progression in mammalian cells from replication fork disruption, such that HDR is required to restart the fork for a proper completion of replication as in *E. coli* (40). Consistent with a similar role in mammalian cells is the colocalization of BRCA1 with PCNA after hydroxyurea treatment of cells (13).

Mice and cells harboring a *Brca1* mutation that deletes exon 11 are considered to be hypomorphic but not null for *Brca1*, because null alleles cause early embryonic lethality, whereas mice with an exon 11 deletion can survive at low frequency on a p53 background (41). These mice have underdeveloped mammary glands, as do mice with an exon 11 deletion specifically targeted to breast tissue, consistent with impaired cellular proliferation (28, 41). It is possible that extended viability results from residual HDR, because, even if diminished, we find that HDR is not completely abrogated by the exon 11 deletion. Although the role of nuclear foci is uncertain, Rad51 foci are also not completely abrogated in this cell line, consistent with residual HDR (17).

Spliced isoforms of *BRCA1* found *in vivo* include *BRCA1Δ11b* and *BRCA1Δ672–4095* (42, 43). Some lack the nuclear localization signals that are present in the 5′ end of exon 11 and are predominantly located in the cytoplasm (42, 43). The cytoplasmic localization of these products would seem to be predictive of a HDR defect, as improper cellular localization of BRCA2 and, surprisingly, Rad51 has been implicated as the mechanism for defective HDR observed in cells with a *BRCA2* mutation (44). The exon 11 splice variants would still be expected to interact with other proteins, such as BARD1 or other BRCA1 RING-interacting proteins and the BRCT interacting proteins, as these interactions involve NH_2- and COOH-terminal sequences, respectively, rather than the central exon 11 encoded sequences (45). Nevertheless, functions arising from these interactions may be compromised through sequestration of these interacting proteins in the cytoplasm. The recently described BRCA1 nuclear export sequence suggests that this protein does not reside solely in the nucleus but may shuttle between the cytoplasm and nucleus (46). However, a direct functional analysis of these endogenous spliced products has not been performed.

Heterozygosity for a *BRCA1* mutation in humans results in a predisposition to early-onset breast and ovarian cancer. This predisposition is incurred when the remaining wild-type allele is lost or mutated, as is the case for classical tumor suppressor genes. A phenotype for the heterozygote state has been inferred for some tumor suppressor gene mutations through a dominant-negative phenotype (47, 48). Evidence for loss of tumor suppression solely from haploinsufficiency is less well documented (49, 50). A heterozygote phenotype for viability or tumorigenesis has not been reported in mice with targeted *Brca1* alleles, and thus far human tumors derived from *BRCA1* mutation carriers consistently reveal a loss of the wild-type allele. However, subtle changes in ovary and breast morphology have been described in mice heterozygous for either *Brca1* or *Brca2* mutations (51). Furthermore, it has been reported that cells from *BRCA1* and *BRCA2* mutation carriers are more radiosensitive than cells from wild-type individuals (24). In our analysis of the $Brca1^{+/-}$ cells, there was no decrease in the ability to gene target, repair a DSB by gene conversion, or maintain genetic integrity or mitomycin-C resistance. However, only partial complementation of repair defects was found with low transgene expression, which measured 10- 20% of wild-type *Brca1* expression. Therefore, the possibility remains that a significant reduction in the expression of *BRCA1* or the presence of dominant-negative

truncated alleles may impart functional consequences that predispose to tumorigenesis, especially under conditions of increased DNA damage or increased proliferation.

We have found that *Brca1*$^{-/-}$ cells exhibit nearly 100-fold sensitivity as compared with the *Brca1*$^{+/+}$ cells after treatment with mitomycin-C at the LD_{50} for wild-type cells. Recently, it was shown that in *Saccharomyces cerevisiae,* the pathways used in the repair of cisplatin-induced interstrand cross-links were cell cycle dependent. The intermediate in the repair of the interstrand cross-links in dividing cells is a DSB that is repaired by homologous recombination (52). Agents that produce DNA interstrand cross-links are some of the most effective antitumor agents in clinical use, although their use is often limited by the toxicity incurred in normal cells. If the preference for HDR in cycling mammalian cells is preserved, it suggests that the exquisite sensitivity of *Brca1*-deficient cells to interstrand cross-linking agents may provide an extremely favorable therapeutic ratio in the treatment of tumors derived from *BRCA1* mutation. This hypothesis can be explored in the recently derived *Brca1*-deficient mouse mammary tumors (28).

The predominant function of BRCA1 that suppresses tumorigenesis has been difficult to determine, likely because of the tightly coordinated functions of DNA damage signaling, repair, and transcriptional regulation of cellular damage response genes. Genes involved in limiting chromosome aberrations would be anticipated to act cooperatively with both cell checkpoints and transcription machinery. An expectation supported by this study is that cells with defective DNA DSB repair develop chromosome instability that leads to a selective advantage either in cell growth or in the suppression of cell death and, ultimately, to tumorigenesis.

ACKNOWLEDGMENTS

We thank Dr. Beverly Koller (University of North Carolina, Chapel Hill, Chapel Hill, NC) for providing the BRCA1$^{-/-}$ 236.44 ES and BRCA1$^{-/-}$, tgt cell lines.

REFERENCES

1. Gowen, L. C., Avrutskaya, A. V., Latour, A. M., Koller, B. H., and Leadon, S. A. BRCA1 required for transcription-coupled repair of oxidative DNA damage. Science (Wash. DC), *281:* 1009–1012, 1998.
2. Moynahan, M. E., Chiu, J. W., Koller, B. H., and Jasin, M. Brca1 controls homology-directed DNA repair. Mol. Cell, *4:* 511–518, 1999.
3. Scully, R., Ganesan, S., Vlasakova, K., Chen, J., Socolovsky, M., and Livingston, D. M. Genetic analysis of BRCA1 function in a defined tumor cell line. Mol. Cell, *4:* 1093–1099, 1999.
4. Cortez, D., Wang, Y., Qin, J., and Elledge, S. J. Requirement of ATM-dependent phosphorylation of BRCA1 in the DNA damage response to double-strand breaks. Science (Wash. DC), *286:* 1162–1166, 1999.
5. Tibbetts, R. S., Cortez, D., Brumbaugh, K. M., Scully, R., Livingston, D., Elledge, S. J., and Abraham, R. T. Functional interactions between BRCA1 and the checkpoint kinase ATR during genotoxic stress. Genes Dev., *14:* 2989–3002, 2000.
6. Lee, J. S., Collins, K. M., Brown, A. L., Lee, C. H., and Chung, J. H. hCds1-mediated phosphorylation of BRCA1 regulates the DNA damage response. Nature (Lond.), *404:* 201–204, 2000.
7. Chai, Y. L., Cui, J., Shao, N., Shyam, E., Reddy, P., and Rao, V. N. The second BRCT domain of BRCA1 proteins interacts with p53 and stimulates transcription from the p21WAF1/CIP1 promoter. Oncogene, *18:* 263–268, 1999.
8. Li, S., Chen, P. L., Subramanian, T., Chinnadurai, G., Tomlinson, G., Osborne, C. K., Sharp, Z. D., and Lee, W. H. Binding of CtIP to the BRCT repeats of BRCA1 involved in the transcription regulation of p21 is disrupted upon DNA damage. J. Biol. Chem., *274:* 11334–11338, 1999.
9. Li, S., Ting, N. S., Zheng, L., Chen, P. L., Ziv, Y., Shiloh, Y., Lee, E. Y., and Lee, W. H. Functional link of BRCA1 and ataxia telangiectasia gene product in DNA damage response. Nature (Lond.), *406:* 210–215, 2000.
10. Wang, Y., Cortez, D., Yazdi, P., Neff, N., Elledge, S. J., and Qin, J. BASC, a super complex of BRCA1-associated proteins involved in the recognition and repair of aberrant DNA structures. Genes Dev., *14:* 927–939, 2000.
11. Shen, S. X., Weaver, Z., Xu, X., Li, C., Weinstein, M., Chen, L., Guan, X. Y., Ried, T., and Deng, C. X. A targeted disruption of the murine *Brca1* gene causes γ-irradiation hypersensitivity and genetic instability. Oncogene, *17:* 3115–3124, 1998.
12. Scully, R., Chen, J., Plug, A., Xiao, Y., Weaver, D., Feunteun, J., Ashley, T., and Livingston, D. M. Association of BRCA1 with Rad51 in mitotic and meiotic cells. Cell, *88:* 265–275, 1997.
13. Scully, R., Chen, J., Ochs, R. L., Keegan, K., Hoekstra, M., Feunteun, J., and Livingston, D. M. Dynamic changes of BRCA1 subnuclear location and phosphorylation state are initiated by DNA damage. Cell, *90:* 425–435, 1997.
14. Zhong, Q., Chen, C. F., Li, S., Chen, Y., Wang, C. C., Xiao, J., Chen, P. L., Sharp, Z. D., and Lee, W. H. Association of BRCA1 with the hRad50-hMre11-p95 complex and the DNA damage response. Science (Wash. DC), *285:* 747–750, 1999.
15. Gowen, L. C., Johnson, B. L., Latour, A. M., Sulik, K. K., and Koller, B. H. Brca1 deficiency results in early embryonic lethality characterized by neuroepithelial abnormalities. Nat. Genet., *12:* 191–194, 1996.
16. Snouwaert, J. N., Gowen, L. C., Latour, A. M., Mohn, A. R., Xiao, A., DiBiase, L., and Koller, B. H. BRCA1 deficient embryonic stem cells display a decreased homologous recombination frequency and an increased frequency of non-homologous recombination that is corrected by expression of a *Brca1* transgene. Oncogene, *18:* 7900–7907, 1999.
17. Bhattacharyya, A., Ear, U. S., Koller, B. H., Weichselbaum, R. R., and Bishop, D. K. The breast cancer susceptibility gene *BRCA1* is required for subnuclear assembly of Rad51 and survival following treatment with the DNA cross-linking agent cisplatin. J. Biol. Chem., *275:* 23899–23903, 2000.
18. Moynahan, M. E., Pierce, A. J., and Jasin, M. BRCA2 is required for homology-directed repair of chromosomal breaks. Mol. Cell, *7:* 263–272, 2001.
19. Moynahan, M. E., and Jasin, M. Loss of heterozygosity induced by a chromosomal double-strand break. Proc. Natl. Acad. Sci. USA, *94:* 8988–8993, 1997.
20. Richardson, C., Moynahan, M. E., and Jasin, M. Double-strand break repair by interchromosomal recombination: suppression of chromosomal translocations. Genes Dev., *12:* 3831–3842, 1998.
21. Pierce, A. J., Johnson, R. D., Thompson, L. H., and Jasin, M. XRCC3 promotes homology-directed repair of DNA damage in mammalian cells. Genes Dev., *13:* 2633–2638, 1999.
22. Essers, J., Hendriks, R. W., Swagemakers, S. M., Troelstra, C., de Wit, J., Bootsma, D., Hoeijmakers, J. H., and Kanaar, R. Disruption of mouse RAD54 reduces ionizing radiation resistance and homologous recombination. Cell, *89:* 195–204, 1997.
23. te Riele, H., Maandag, E. R., Clarke, A., Hooper, M., and Berns, A. Consecutive inactivation of both alleles of the *pim-1* proto-oncogene by homologous recombination in embryonic stem cells. Nature (Lond.), *348:* 649–651, 1990.
24. Foray, N., Randrianarison, V., Marot, D., Perricaudet, M., Lenoir, G., and Feunteun, J. γ-rays-induced death of human cells carrying mutations of *BRCA1* or *BRCA2*. Oncogene, *18:* 7334–7342, 1999.
25. Liu, N., Lamerdin, J. E., Tebbs, R. S., Schild, D., Tucker, J. D., Shen, M. R., Brookman, K. W., Siciliano, M. J., Walter, C. A., Fan, W., Narayana, L. S., Zhou, Z. Q., Adamson, A. W., Sorensen, K. J., Chen, D. J., Jones, N. J., and Thompson, L. H. XRCC2 and XRCC3, new human Rad51-family members, promote chromosome stability and protect against DNA cross-links and other damages. Mol. Cell, *1:* 783–793, 1998.
26. De Silva, I. U., McHugh, P. J., Clingen, P. H., and Hartley, J. A. Defining the roles of nucleotide excision repair and recombination in the repair of DNA interstrand cross-links in mammalian cells. Mol. Cell. Biol., *20:* 7980–7990, 2000.
27. Xu, X., Weaver, Z., Linke, S. P., Li, C., Gotay, J., Wang, X. W., Harris, C. C., Ried, T., and Deng, C. X. Centrosome amplification and a defective G_2-M cell cycle checkpoint induce genetic instability in BRCA1 exon 11 isoform-deficient cells. Mol. Cell, *3:* 389–395, 1999.
28. Xu, X., Wagner, K. U., Larson, D., Weaver, Z., Li, C., Ried, T., Hennighausen, L., Wynshaw-Boris, A., and Deng, C. X. Conditional mutation of Brca1 in mammary epithelial cells results in blunted ductal morphogenesis and tumour formation. Nat. Genet., *22:* 37–43, 1999.
29. Cui, X., Brenneman, M., Meyne, J., Oshimura, M., Goodwin, E. H., and Chen, D. J. The *XRCC2* and *XRCC3* repair genes are required for chromosome stability in mammalian cells. Mutat. Res., *434:* 75–88, 1999.
30. Yu, V. P., Koehler, M., Steinlein, C., Schmid, M., Hanakahi, L. A., van Gool, A. J., West, S. C., and Venkitaraman, A. R. Gross chromosomal rearrangements and genetic exchange between nonhomologous chromosomes following *BRCA2* inactivation. Genes Dev., *14:* 1400–1406, 2000.
31. Caldecott, K. W., and Jeggo, P. A. Cross-sensitivity of γ-ray-sensitive hamster mutants to cross-linking agents. Mutat. Res., *255:* 111–121, 1991.
32. Kemp, L. M., and Jeggo, P. A. Radiation-induced chromosome damage in X-ray-sensitive mutants (xrs) of the Chinese hamster ovary cell line. Mutat. Res., *166:* 255–263, 1986.
33. Karanjawala, Z. E., Grawunder, U., Hsieh, C. L., and Lieber, M. R. The nonhomologous DNA end joining pathway is important for chromosome stability in primary fibroblasts. Curr. Biol., *9:* 1501–1504, 1999.
34. Difilippantonio, M. J., Zhu, J., Chen, H. T., Meffre, E., Nussenzweig, M. C., Max, E. E., Ried, T., and Nussenzweig, A. DNA repair protein Ku80 suppresses chromosomal aberrations and malignant transformation. Nature (Lond.), *404:* 510–514, 2000.
35. Gao, Y., Ferguson, D. O., Xie, W., Manis, J. P., Sekiguchi, J., Frank, K. M., Chaudhuri, J., Horner, J., DePinho, R. A., and Alt, F. W. Interplay of p53 and DNA-repair protein XRCC4 in tumorigenesis, genomic stability and development. Nature (Lond.), *404:* 897–900, 2000.
36. Griffin, C. S., Simpson, P. J., Wilson, C. R., and Thacker, J. Mammalian recombination-repair genes *XRCC2* and *XRCC3* promote correct chromosome segregation. Nat. Cell Biol., *2:* 757–761, 2000.
37. Tutt, A., Gabriel, A., Bertwistle, D., Connor, F., Paterson, H., Peacock, J., Ross, G., and Ashworth, A. Absence of Brca2 causes genome instability by chromosome breakage and loss associated with centrosome amplification. Curr. Biol., *9:* 1107–1110, 1999.

38. Gottifredi, V., Shieh, S. Y., Taya, Y., and Prives, C. p53 accumulates but is functionally impaired when DNA synthesis is blocked. Proc. Natl. Acad. Sci. USA, *98:* 1036–1041, 2001.
39. Johnson, R. D., and Jasin, M. Sister chromatid gene conversion is a prominent double-strand break repair pathway in mammalian cells. EMBO J., *19:* 3398–3407, 2000.
40. Marians, K. J. PriA-directed replication fork restart in *Escherichia coli*. Trends Biochem. Sci., *25:* 185–189, 2000.
41. Cressman, V. L., Backlund, D. C., Avrutskaya, A. V., Leadon, S. A., Godfrey, V., and Koller, B. H. Growth retardation, DNA repair defects, and lack of spermatogenesis in BRCA1-deficient mice. Mol. Cell. Biol., *19:* 7061–7075, 1999.
42. Thakur, S., Zhang, H. B., Peng, Y., Le, H., Carroll, B., Ward, T., Yao, J., Farid, L. M., Couch, F. J., Wilson, R. B., and Weber, B. L. Localization of BRCA1 and a splice variant identifies the nuclear localization signal. Mol. Cell. Biol., *17:* 444–452, 1997.
43. Wilson, C. A., Payton, M. N., Elliott, G. S., Buaas, F. W., Cajulis, E. E., Grosshans, D., Ramos, L., Reese, D. M., Slamon, D. J., and Calzone, F. J. Differential subcellular localization, expression and biological toxicity of BRCA1 and the splice variant BRCA1-δ11b. Oncogene, *14:* 1–16, 1997.
44. Davies, A. A., Mason, J-Y., McIlwraith, M. J., Stasiak, A. Z., Venkitaraman, A. R., and West, S. C. Role of BRCA2 in control of the Rad51 recombination and DNA repair protein. Mol. Cell, *4:* 273–282, 2001.
45. Deng, C. X., and Brodie, S. G. Roles of *BRCA1* and its interacting proteins. Bioessays, *22:* 728–737, 2000.
46. Rodriguez, J. A., and Henderson, B. R. Identification of a functional nuclear export sequence in BRCA1. J. Biol. Chem., *275:* 38589–38596, 2000.
47. Gualberto, A., Aldape, K., Kozakiewicz, K., and Tlsty, T. D. An oncogenic form of p53 confers a dominant, gain-of-function phenotype that disrupts spindle checkpoint control. Proc. Natl. Acad. Sci. USA, *95:* 5166–5171, 1998.
48. Blandino, G., Levine, A. J., and Oren, M. Mutant p53 gain of function: differential effects of different p53 mutants on resistance of cultured cells to chemotherapy. Oncogene, *18:* 477–485, 1999.
49. Fero, M. L., Randel, E., Gurley, K. E., Roberts, J. M., and Kemp, C. J. The murine gene *p27Kip1* is haplo-insufficient for tumour suppression. Nature (Lond.), *396:* 177–180, 1998.
50. Venkatachalam, S., Shi, Y. P., Jones, S. N., Vogel, H., Bradley, A., Pinkel, D., and Donehower, L. A. Retention of wild-type p53 in tumors from p53 heterozygous mice: reduction of p53 dosage can promote cancer formation. EMBO J., *17:* 4657–4667, 1998.
51. Bennett, L. M., McAllister, K. A., Malphurs, J., Ward, T., Collins, N. K., Seely, J. C., Gowen, L. C., Koller, B. H., Davis, B. J., and Wiseman, R. W. Mice heterozygous for a *Brca1* or *Brca2* mutation display distinct mammary gland and ovarian phenotypes in response to diethylstilbestrol. Cancer Res., *60:* 3461–3469, 2000.
52. McHugh, P. J., Sones, W. R., and Hartley, J. A. Repair of intermediate structures produced at DNA interstrand cross-links in *Saccharomyces cerevisiae*. Mol. Cell. Biol., *20:* 3425–3433, 2000.

HOMOLOGY-DIRECTED REPAIR AS A SAFEGUARD OF GENOME INTEGRITY IN MAMMALIAN CELLS

Mary Ellen Moynahan, Roger Johnson, Andrew Pierce, Tracy Cui, & Maria Jasin, Memorial Sloan-Kettering Cancer Center, NYC, NY

DNA repair processes play an essential role in maintaining chromosome structure and genetic integrity. The significance of these processes is emphasized as defects in DNA repair pathways are linked to human disease and malignancy. A DNA double-strand break (DSB) is one type of lesion that can compromise genomic integrity. Two major pathways are responsible for the repair of DSBs in mammalian cells, nonhomologous and homologous repair (Liang et al., PNAS 95, 5172 *1998*). A role for nonhomologous repair is well established, whereas a role for homologous repair is just emerging. We have recently demonstrated that homologous repair from a sister-chromatid is extremely efficient (Johnson & Jasin, submitted). Recombination between homologous chromosomes (Moynahan & Jasin, PNAS 94, 8988 *1997*) or homologous sequences on heterologous chromosomes (Richardson et al., Genes Dev., 12, 3831 *1998*) can also be used to repair a DSB, although with a significantly reduced efficiency.

An essential component of homologous recombination pathways is the evolutionarily conserved strand transferase protein, yeast Rad51. Several mammalian proteins have been implicated in homologous recombination based on their homology to Rad51, including a mammalian Rad51 homolog which is about 68% identical to the yeast protein, and the distantly related XRCC2 and XRCC3 proteins, which share about 20% identity with human Rad51 (Liu et al. Mol. Cell 1, 783 *1998*). We have recently shown that cell lines with mutated *XRCC2 or XRCC3* genes have reduced homologous repair (Johnson et al. Nature 401, 397 1999; Pierce et al., Genes Dev. 13, 2633, *1999*). The products of the hereditary breast cancer genes *BRCA1* and *BRCA2* are also implicated in the Rad51 homologous pathway, as they have been shown to associate with Rad51. Examination of DSB repair in cells with hypomorphic *BRCA1* or *BRCA2* alleles has also demonstrated reduced homologous repair (Moynahan et al., Mol. Cell. 4, 511, *1999*). As each of these mutant cell lines exhibit chromosome abnormalities, homologous repair can be concluded to have a key role in maintaining genomic integrity in mammalian cells. The demonstration of homologous repair defects in BRCA-deficient lines strongly suggests a link between such repair defects and tumorigenesis.

Homologous Recombination, Genomic Integrity, and Cancer

Mary Ellen Moynahan, Jeremy Stark, Roger Johnson, Ulrica Westermark, and Maria Jasin. Memorial Sloan-Kettering Cancer Center, New York NY

A number of DNA repair genes have been classified as genomic "caretakers" in that they protect cells from becoming tumorigenic by preventing the accumulation of mutations. One type of DNA damage is a chromosomal double-strand break (DSB) which can be formed by radiation treatment, oxygen free-radicals, topoisomerase failure, and, possibly most commonly, DNA replication. Considering the possible mutability of unrepaired or misrepaired DSBs, genes involved in DSB repair could be predicted to play a genomic caretaker role in the cell.

In mammalian cells, both homologous and nonhomologous repair are employed to repair DSBs. We have recently obtained evidence that genes that suppress tumorigenesis function in DSB repair, in particular homology-directed repair (HDR) by gene conversion. The products of the hereditary breast cancer susceptibility genes *BRCA1* and *BRCA2* have been shown to interact with RAD51 directly through protein-protein interactions or indirectly in nuclear foci. We determined that murine embryonic stem (ES) cell lines containing hypomorphic alleles of *Brca1* or *Brca2* exhibit HDR defects, such that DSB-promoted gene conversion is reduced 5 to 6-fold. Evidence suggests that a larger decrease in the frequency of HDR would be expected in cells which have null alleles for either of these genes. The hypomorphic allele for *Brca1* we tested results in a splice variant in which exon 11 is skipped, deleting approximately half of the coding sequence. Mice containing a similar allele have been found by Xu et al. (*Nat. Gen.* 22, 37-44; 1999) to develop mammary tumors. In addition to HDR defects, the *Brca1* mutant ES cells are mildly sensitive to ionizing radiation but profoundly sensitive to mitomycin C. These cells also exhibit a high frequency of spontaneous chromosome aberrations, possibly from damage arising during DNA replication. Repair phenotypes return to wild-type levels when a *Brca1* allele is corrected by gene targeting to restore the exon 11 sequences.

Thus, the *Brca1* (and *Brca2*) mutants together with other HDR mutants (*XRCC2* and *XRCC3*) define the mammalian phenotype arising from defective homologous repair, in terms of sensitivity to DNA damaging agents and genomic instability. The correlation between this defective HDR phenotype and tumorigenesis is striking and suggests that genes involved in homologous repair are *bona fide* caretaker genes. This is further supported by a recent study in which we found that tumorigenesis in $Rb^{+/-}$ mutant mice is potentiated by mutation of another gene involved in homologous recombination *Rad54*. In the case of the hereditary breast cancer genes, a causal role for the HDR defects of *Brca1* or *Brca2* mutants in promoting tumorigenesis remains to be conclusively established, as both proteins have a number of interacting partners with roles in other cellular processes.